BNL 713 (T-250)

THE SETTLED BED FAST REACTOR STATUS REPORT

W.A. ROBBA, Editor

January 20, 1962

BROOKHAVEN NATIONAL LABORATORY
ASSOCIATED UNIVERSITIES, INC.
under contract with the
UNITED STATES ATOMIC ENERGY COMMISSION

DISCLAIMER

BNL 713 (T-250)
(Reactor Technology – TID-4500, 17th Ed.)

THE SETTLED BED FAST REACTOR STATUS REPORT

W.A. ROBBA, Editor

Report written by

ARNOLD ARONSON
LEON GREEN
LORANUS P. HATCH
KENNETH C. HOFFMAN
MELVIN LEVINE
JAMES MCNICHOLAS
GUYON PANCER
WILLIAM A. ROBBA

This is an informal progress report. The results and data presented are preliminary and subject to change. In the interests of rapid publication, editorial work has been necessarily limited.

January 20, 1962

BROOKHAVEN NATIONAL LABORATORY
UPTON, NEW YORK

LEGAL NOTICE

PRINTED IN USA
PRICE $2.25

Available from the
Office of Technical Services
Department of Commerce
Washington 25, D.C.

March 1962 1050 copies

TABLE OF CONTENTS

LIST OF FIGURES

LIST OF TABLES

SUMMARY

This report represents a continuation of the effort on large power reactor systems utilizing settled bed fuels. The previous study (BNL-5372)* consisted of an evaluation of a number of systems both thermal and fast. This included a UO_2-Sodium-Graphite Thermal Reactor, a U^{233}-Li^7-BeO Thermal Breeder, a Sodium Cooled Fast Reactor with internal heat exchanger, and two types of Directly Cooled Fast Reactors. As a result of this study it was decided to investigate further the directly cooled fast concept. The reason for this choice was dictated primarily by the greater simplicity of the directly cooled fast systems and the greater cost reduction potential. It is admittedly true that these factors may have resulted in part from the fact that the systems have not been investigated in much detail. As a consequence this study has concentrated more on the stability of the reactors and paid more attention to design features, heat transfer, fluid flow and fuel cycle problems. In addition to further assess the potential, the sodium outlet temperature has been raised from 1050°F to 1200°F and the electrical power output has been increased from 300 MWe net to 360 MWe. This was done to permit mating the reactor to a modern efficient steam electric power plant. We have also used more recent values, based

* Preliminary Report - Internal Distribution Only

on the Fermi plant, to estimate capital costs of the reactor systems.

The fuel cycle costs obtained for these reactors are quite low, falling below 1 mill/kwh at maximum burnups in excess of 40,000 to 50,000 MWD/MT. Power generation costs range from 5.3 to 6.2 mills/kwh depending upon the burnups attainable. No optimization of these systems has yet been undertaken so these numbers are still very preliminary.

As pointed out in the previous report the feasibility of the fuel cycle has yet to be demonstrated. An experimental program to determine feasibility is underway but has not progressed to the point where definitive results have been obtained. The program consists primarily of out-of-pile and in-pile tests of the carbide fuel system. It is important to point out that the results obtained from this program are of use in demonstrating the fuel concept and are not restricted to any specific reactor type. Carbide fuel has been specified for the fast reactor system in preference to the oxide because of the higher thermal conductivity of the carbide. Though the final proof must await the outcome of parametric type surveys and optimization studies, it is known that for <u>equal</u> size cores the carbide fuel will have higher performance and better economics than an oxide if both are taken to equal burnup. It is possible to use the oxide fuel as an alternate in the radial flow designs with a resulting lower power density and higher pressure

drop. Metal alloy fuels were briefly investigated on the basis of better heat transfer characteristics, neutron economics and lower fabrication costs. It was originally thought that a $5-10/kg fabrication cost was possible. This represents a considerable cost savings over the $60/kg charge used in our studies for ceramic fuels. However, it was found that the low costs applied to un-alloyed uranium particles not uranium-plutonium molybdenum alloy spherical pellets. Estimates of $30/kg were obtained for this fuel and on the basis of 5,000 MWD/T maximum burnup as compared with 50,000 MWD/T maximum for the ceramics the use of metal fuels appears rather unattractive.

It should be noted that the emphasis in the study is placed on the reactor and its internals since it is in this area that the settled bed reactor differs from a sodium cooled solid fuel reactor. Components and equipments external to the reactor would be similar to those ascribed to a large sodium cooled nuclear power plant. The decision to do further design work on the directly cooled fast reactor implies that with unclad fuel the primary sodium loop will be contaminated to an extent which is presently unknown. This factor will not greatly affect the shield design of the primary sodium loop since the sodium will be highly radioactive anyway. The contamination will, however, have an effect on maintenance procedures and this is accounted for in O & M charges. The use of clad fuel pellets would alleviate this problem to a considerable

extent but would also result in somewhat higher fabrication costs. Concept feasibility is dependent upon successful cladding techniques only if the cladding is necessary to insure pellet integrity over fuel lifetime. The problem of sintering or sticking of the fuel pellets becomes serious only if this occurs in a short time period (i.e., less than two weeks) during the lifetime of the fuel in a reactor cycle. The reason for this is that even though the major part of the fuel resides in the reactor for a 24-month or longer period, fuel removal, addition and mixing by fluidization may occur every two to four weeks, thus preventing agglomeration. The experimental program must determine the relation between sintering time and irradiation time, if such exists, since it is possible that the sintering time may be much shorter after long time irradiation.

In addition to criticality calculations and flux distributions appreciable effort was devoted to calculating sodium coefficients, bed settling coefficients and control rod effectiveness, particularly in the central pipe of the radial flow reactors. Unfortunately, time did not permit the use of two dimensional codes so that the results presented may change as the work is refined. It is also evident when one reviews the economic section that physics parametric studies are needed to determine optimum sizes and breeding ratios. Sodium coefficients are mildly positive for the large axial core and negative for the radial cores. A dollar's worth of reac-

tivity is equivalent to a 20% decrease in sodium density for the axial core and ~5% and 11% increase in sodium density for the radial carbide and radial oxide cores respectively. Bed compaction coefficients are all positive and because of this a critical problem in the development program is to find a method of achieving a stable settled bed configuration. The fact that these coefficients vary in either sign and magnitude or in magnitude indicates that these effects can be minimized by choice of core size and configuration. A considerable amount of analysis remains to be done in this area.

Heat transfer and fluid flow analyses have been further refined. Thermal stresses in fuel, boiling of sodium in a hot sector and pressure drop through the core are the major design limits. These calculations have been done for a few specific core configurations and parametric studies in conjunction with physics and economic estimates must now be initiated in order to establish optimum conditions.

Mechanical design work was performed on the radial flow concept since it is somewhat more complex internally than the axial design but thermal stress analysis and expansion problems have not been investigated in detail.

INTRODUCTION

This report presents the status of work on fast reactor systems utilizing fuel in the form of particulate solids and cooled by direct flow of sodium through a settled bed of such fuel. The fuel is in a settled and static condition during operation with the flow of coolant in such a direction as to maintain the fuel in the settled state. The fuel is fluidized by pumping sodium up through the bed and during this state removal, addition and mixing of fuel is accomplished. During operations of this type the reactor is in a shut down condition. The ability to operate the reactor at power with the fuel all in the core in a static condition, yet handle fuel as a liquid during transfer and redistribution operations is one of the major advantages of this system.

In the axial type core sodium flow is downward through the bed during power operation. The core is a right cylinder with height equal to 0.6 the diameter to reduce pressure drop. A blanket of similar fuel particles surrounds the core and is cooled by down flowing sodium. Flow is reversed for fluidizing operations.

The radial flow core is cooled by bringing sodium into a central pipe from whence it flows radially outward through core and blanket. In the top portions of the core the sodium flow has

a vertical component to prevent lifting the bed in these regions. Separate sodium lines are required to establish up flow during fluidization operations. The main advantage of the radial core is its lower pressure drop. This permits a smaller core and a lower inventory.

General characteristics of the fuel cycle are listed below:

a. Maintenance of uniform distribution of the fuel-containing solids, and, therefore, of the fuel density, throughout the entire core.

b. Overall mobility in the fuel permitting the particle suspension to flow freely in tubes connecting the reactor core region with an outside vessel (for fuel makeup and reprocessing) in response to pressure adjustment in the fluidizing liquid stream. Provision for fuel makeup at frequent intervals is itself an important advantage since only small amounts of excess reactivity would then be required. This is extremely important in a fast reactor.

c. Elimination of excessive fabrication costs commonly associated with the manufacture of solid fuel elements under close tolerance requirements. The cost of coating fuel particles is not taken into account here since any coating process must at present be considered an

expensive one. The containment of the fission products within the fuel particles by means of applied coatings would provide a valuable additional degree of freedom in the reactor design since the problems associated with separation of fuel and coolant would then be minimized. The economic aspects of particle coating processes and the overall influence on fuel cycle (including reprocessing) and maintenance costs is presently unknown.

d. Excellent possibility of very high burnup in the fuel.

e. Ease of reprocessing of the fuel due to the ability to transfer the fluidized fuel in the same manner that a liquid is transferred.

f. Assurance of achieving uniform burnup in the fuel by virtue of the mobility of the fuel.

g. Confinement of the fuel to the core of the reactor while retaining the other advantages of a liquid fuel.

h. Use of the particulate form of solid fuel without the need to recirculate the fuel through pumps, valves, etc., and without problems of erosion or attrition of fuel particles. Even with fluidization of the fuel almost quiescent conditions obtain with the laminar flow state.

THE CARBIDE FUEL PROGRAM

The proposed fuel for this reactor is a uranium-plutonium-carbide fuel in the form of 1/8-inch diameter unclad spherical particles. Uranium-plutonium-oxide is being considered as a possible alternative. The development work with carbide fuel up to the present has centered on clad pellets and rods, and no attempt has been made to fabricate U-Pu-C spheres in the 1/8-inch diameter size range. Actually the general development of U-Pu-C fuel is still in its infancy. Until more basic data are obtained on this three-component system, the Brookhaven National Laboratory fuel program would utilize uranium carbide. In preparation for such a fuel development program a review of the state of the art regarding uranium carbide and uranium-plutonium-carbide technology was made and the availability of the fuel material was investigated. Three general aspects were considered: fabrication technique, fuel composition, and radiation damage. A program for out-of-pile and in-pile testing is presented.

Fabrication Techniques.

There are two basic methods of fabrication of both uranium carbide and plutonium carbide fuel being employed at the present time. They are powder metallurgy and arc melting and casting. Material fabricated by either method has both advantages and disadvantages which appear to be strongly dependent on its specific application to a particular reactor system. No selection

of fabrication technique can be made at this time with reference to the settled bed fast breeder reactor. In the final analysis, the size and shape of the fuel required for this reactor may be the governing factor in selecting the fabrication technique.

Composition of Fuel

The ideal composition of any carbide fuel (UC or PuC) is one which contains stoichiometric carbon, (4.8 w/o C). However, from practical considerations it is not economically feasible to obtain this exact carbon to uranium ratio. Therefore, with these fuels we would be dealing with either hypostoichiometric (<4.8 w/o C) or hyperstoichiometric (>4.8 w/o C).

HYPOSTOICHIOMETRIC CARBIDE FUEL

The hypostoichiometric fuel would have a mixture of uranium carbide and free uranium (UC + U), and thus have a self-imposed temperature limitation based on the melting point of uranium. In addition, the presence of free uranium might lead to radiation instability. However, present radiation damage studies on hypostoichiometric fuel has not revealed this effect. Also, out-of-pile studies indicate that there is no reaction with sodium. Within the temperature limitations, the material appears to behave as if it were stiochiometric uranium carbide.

HYPERSTOICHIOMETRIC CARBIDE FUEL

The hyperstoichiometric fuel is a mixture of uranium

carbide, uranium dicarbide, uranium sesquicarbide (UC, UC_2 and U_2C_3). Out-of-pile experiments indicate that a decarburization reaction occurs between the UC_2 and sodium or NaK, and that with a 1000°-1200°F liquid metal temperature, continued exposure would result in complete decarburization of the fuel. The depth of decarburization appears to be independent of specimen diameter and carbon content. Since the decarburization process results in an increase in carbon content in the liquid metal, a corresponding carburization of stainless steel components in contact with the liquid metal would occur.

Recent work at AI has indicated that heat treatment of the hyperstoichiometric uranium carbide fuel may result in a conversion of the UC_2 to U_2C_3 which appears to be more stable against decarburization. However, more experimental data on this conversion is required.

Plutonium Carbide Fuels

There is some information available on PuC fuel which may have significant bearing on the UC-PuC fuel. When considering hypostoichiometric PuC one encounters the same problem as with UC. The melting point of Pu is only 640°C (1180°F). This is well below the average surface temperature of the fuel, and, as a result, complete melting of all free plutonium present in the fuel would probably occur. Hyperstoichiometric fuel appears to be com-

posed of PuC-Pu_2C_3 which, if one assumes a similarity to the UC-U_2C_3 system, should be stable against decarburization.

Plutonium-Uranium Carbide Fuel

At this early stage of the development of the three component fuel system, it is difficult to specify the most desirable composition of the fuel. However, it will probably be in the range of 80 w/o UC - 20 w/o PuC. On considering the three phase system there may be a decided advantage in using the hypostoichiometric fuel. If a U-Pu phase results from the excess metal the possibility of free plutonium is eliminated. One must still consider the properties of the U-Pu phase and free uranium under high temperature and radiation. However, as indicated above, the presence of free uranium does not appear to be as detrimental as one might assume.

RADIATION DAMAGE

An extensive radiation damage study program with UC is now in progress at BMI, NDA, and AI. In addition both NDA and ANL are engaged in an irradiation program with U-Pu-C fuel systems. However, there are no data available on the latter system at the present time.

An examination of the various in-pile UC fueled capsules at BMI reveal very little damage at burnups up to 25,000 Mwd/ton. There is no indication as to which fabrication technique appears to give the best results. Very high burnups (100,000 Mwd/ton)

may cause an increase in volume. The feasibility of obtaining this high a burnup level is unknown at this time.

Anticipating radiation damage data on the U-Pu-C system, some investigators feel that the U-Pu phase in hypostoichiometric fuel may be somewhat unstable.

Out-Of-Pile Testing

As part of the development program of the reactor fuel system, a series of out-of-pile capsule tests will be performed. These tests will serve a three-fold purpose:

1. To screen fuel materials fabricated by the various methods and to determine the most promising fuel composition;
2. To investigate the possibility of sintering between the spherical fuel particles in the presence of high temperature liquid metals;
3. To provide control specimens for comparison with results of in-pile tests in order to delineate between thermal and radiation effects.

The capsule design is shown in Figure 1 and a photograph of the assembled capsule and its components are shown in Figures 2 and 3 respectively. The 0.125-inch spherical fuel particles will be placed in the inner tube (0.180-inch ID), thereby essentially forming a column of fuel. The function of the hole pattern on the tube is to allow the liquid metal in the central

ITEM	QUAN.	NAME	MATERIAL OR DRAWING NO.
1	1	1" PIPE SCH. 10S × 8 1/8"	ST. ST'L TYPE 304
2	1	1 1/2" PIPE SCH. 10S × 3"	ST. ST'L TYPE 304
3	1	1 1/2"-2000 # SOC. WELD CAP	ST. ST'L TYPE 304
4	1	1 1/2" × 1" REDUCER SCH. 10S	ST. ST'L TYPE 304
5	1	.250 O.D. × .035 WALL TUBE × 12 1/2"	ST. ST'L TYPE 304
6	1	.250 O.D. × .035 WALL TUBE × 12"	ST. ST'L TYPE 304
7	1	.375 O.D. × .049 WALL TUBE × 1 1/2"	ST. ST'L TYPE 304
8	1	.375 O.D. × .049 WALL TUBE × 1/2"	ST. ST'L TYPE 304
9	1	.157 DIA. ROD × 6 1/2"	ST. ST'L TYPE 303
10	1	.157 DIA. ROD × 3/4	ST. ST'L TYPE 308
11	2	SPACER	SEE DETAIL
12	1	WEIGHT	SEE DETAIL
13	1	END PLATE	SEE DETAIL
14	1	THERMOCOUPLE- CONAX CAT. NO. INC 12K-U	
15	1	SWAGELOK FITTING CAT. NO. 200-1-2W-304	

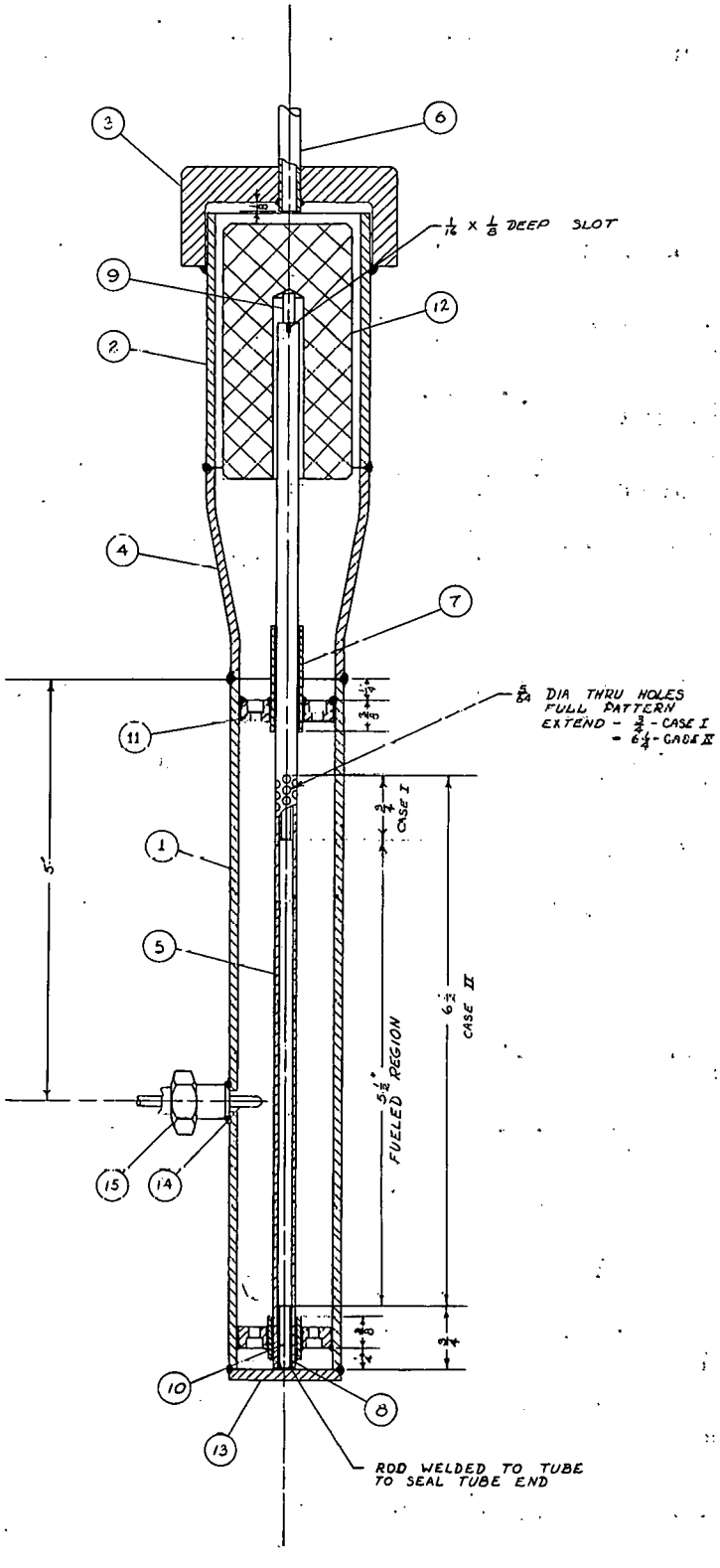

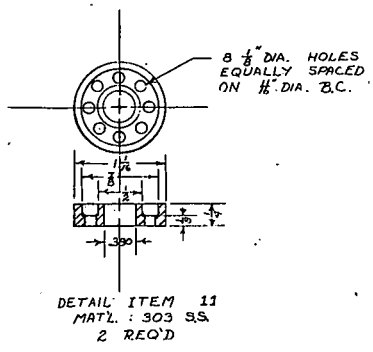

DETAIL ITEM 11
MAT'L. : 303 S.S.
2 REQ'D

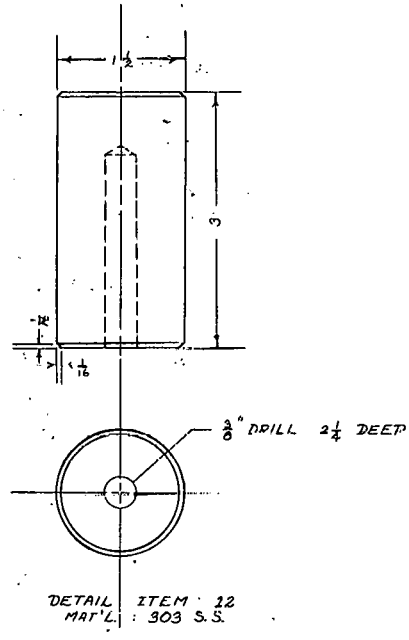

DETAIL ITEM 12
MAT'L. : 303 S.S.

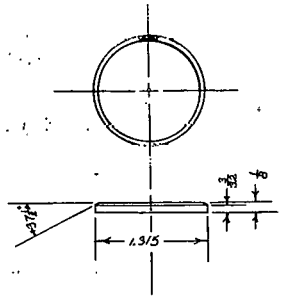

DETAIL ITEM 13
MAT'L. : 304 S.S.

Figure 1. Out-of-pile fuel development capsule.

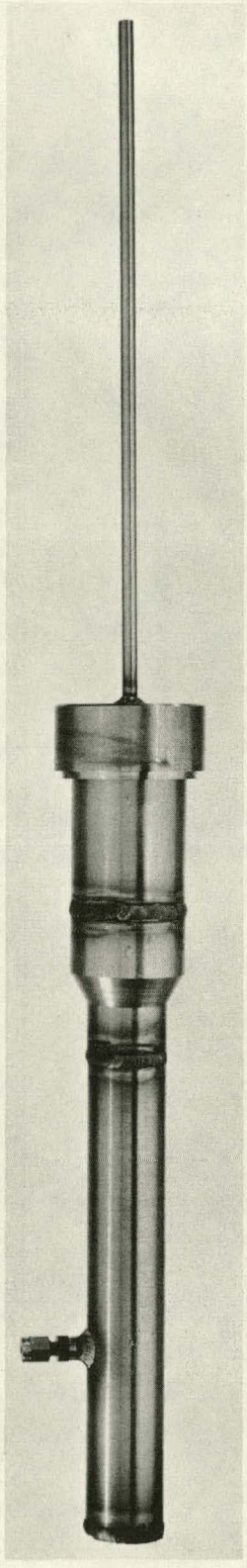

Figure 2. Assembled out-of-pile fuel development capsule.

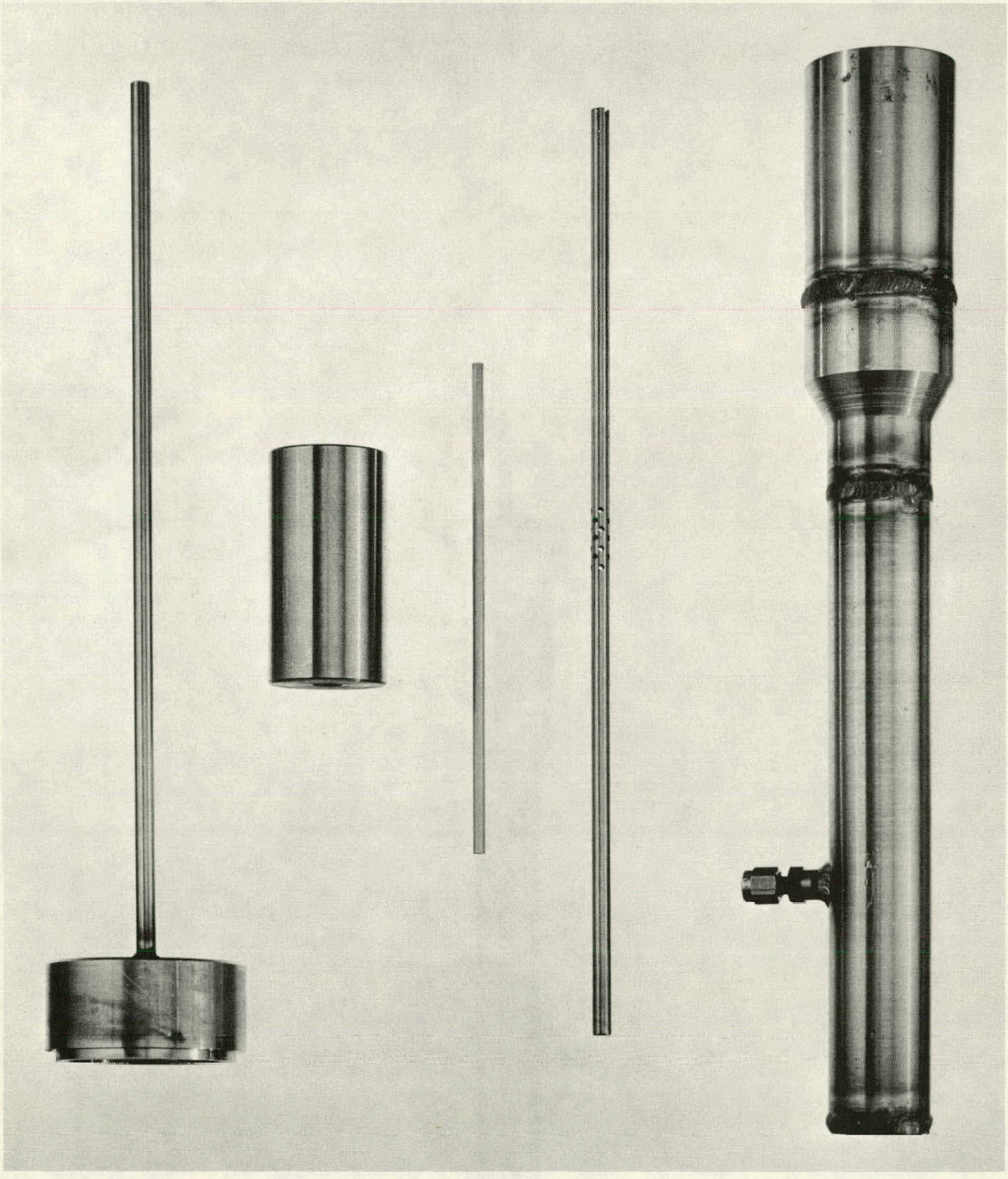

Figure 3. Components of out-of-pile fuel development capsule.

tube to expand into the liquid metal reservoir surrounding it. A dead weight of approximately one pound is transmitted to the fuel by the short solid rod producing forces between particles to approximate those that would be present in the reactor.

The out-of-pile capsule work will be performed with NaK rather than with sodium as the fluid. Initial tests will utilize uranium carbide. The tests will be extended to include uranium-plutonium-carbide when this material is more readily available. The first series of tests to be performed are outlined in Table 1.

TABLE 1

OUT-OF-PILE CAPSULE TEST PROGRAM SERIES I

Capsule designation	Operating temperature, °F	Coolant	Time, Hr
OP-1	1450-1500	NaK	700
OP-2*	300-1450	NaK	700
OP-3	1450-1500	NaK	3000

*Continuous thermal cycle between 300° and 1450°F.

In-Pile Capsule Studies

The in-pile irradiation tests will be required in order to investigate the overall radiation stability of the fuel including swelling, particle breakup, fission gas release, as well as the possibility of sintering of the fuel particles in a high temperature-high radiation environment. In addition, the fuel fabrication

techniques and various fuel compositions which are still acceptable after out-of-pile testing will be further evaluated. The program will be initiated with instrumented capsules using enriched uranium carbide as the fuel material. The final in-pile tests, however, will utilize the uranium-plutonium carbide fuel system. Most of the testing will be performed with a thermal flux as the reference flux. The final in-pile capsules and loop may require radiation in a fast flux. The use of a thermal flux as a basis for investigating the radiation damage can be justified because damage caused by high energy neutrons (~ 0.5 Mev) is insignificant compared to that caused by the phenomena of fission.

One of the major problems associated with settled bed reactor systems is the possible sintering of the fuel particles during power operation. At the present time it is estimated that full power operation cycle for the radial flow fast reactor is approximately one month. At the end of the operation cycle the core fuel would be fluidized for fuel charging or redistribution. It is proposed, therefore, to investigate the condition of the fuel after a capsule irradiation equivalent to one month of full power reactor operation. The fuel will be irradiated for a predetermined period such that the total burnup is the same as that in the reactor system after a one month full power operation cycle. During this radiation period, an applied force between fuel particles will be maintained to simulate the condition in the reactor. Additional capsule tests

will be carried out to obtain high burnup information.

The proposed irradiation tests with enriched uranium carbide will be performed in the BNL graphite reactor and MTR. The capsule design will be such that it will be adaptable to either reactor. The BNL radiation test will provide the necessary low burnup data while the MTR radiation test will provide the burnup data for the one month operating cycle of the proposed radial flow reactor, as well as the required high burnup information.

BNL IN-PILE CAPSULE ASSEMBLY

The conceptual design of the in-pile capsule and thimble has been completed and the final design of the complete assembly is now in progress. The capsule, Figure 4, is a double container unit with a maximum OD of 1-1/8 inch. The OD was fixed to conform to the MTR requirements. The double container concept is necessary to maintain the integrity of the pile in the event of a failure of the inner container with a subsequent release of liquid metal and fuel. The space between the inner and outer container is filled with He at a slight positive pressure. The He will be continually monitored for fission product gases to insure the integrity of the fueled inner container. The uranium carbide spheres will be located in the inner container in a manner identical to that of the out-of-pile capsule, the fueled length being approximately 4 inches. However, the hole pattern is drilled the full fuel length. The purpose of this modifi-

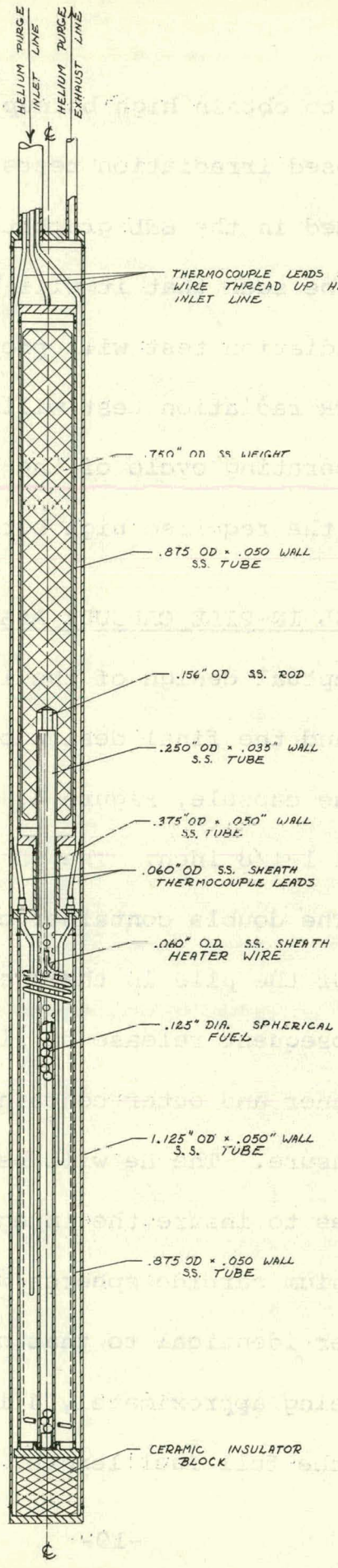

Figure 4. Conceptual design of BNL in-pile capsule.

cation is to eliminate the possibility of a liquid metal void forming in the central tube as a result of a sudden change in heat generation. A heater and thermocouple will be located in the liquid metal bath surrounding the fuel. A dead weight system similar to that in the out-of-pile capsule will again be used to simulate forces between particles. The capsule will be located in a 3-inch vertical hole to be drilled in the BNL Graphite Reactor. Air will be used to cool the capsule which may necessitate finning the outer container. However, these fins will not be necessary for the water-cooled MTR, thereby maintaining the 1-1/8 inch OD capsule requirement. The conceptual design of the thimble shown in Figure 5 includes the required concrete shield plug, air cooling system and instrument train.

Included in Table 2 are the major parameters and some of the details of the capsule.

TABLE 2

BNL IN-PILE CAPSULE PARAMETERS

Fuel	1/8-inch diameter UC spheres
Enrichment	~ 25%
Fuel Surface Temperature	~ 1400°F
Fuel Center Temperature (calc.)	~ 1450°F
Mass of Fuel	10.3 gms UC

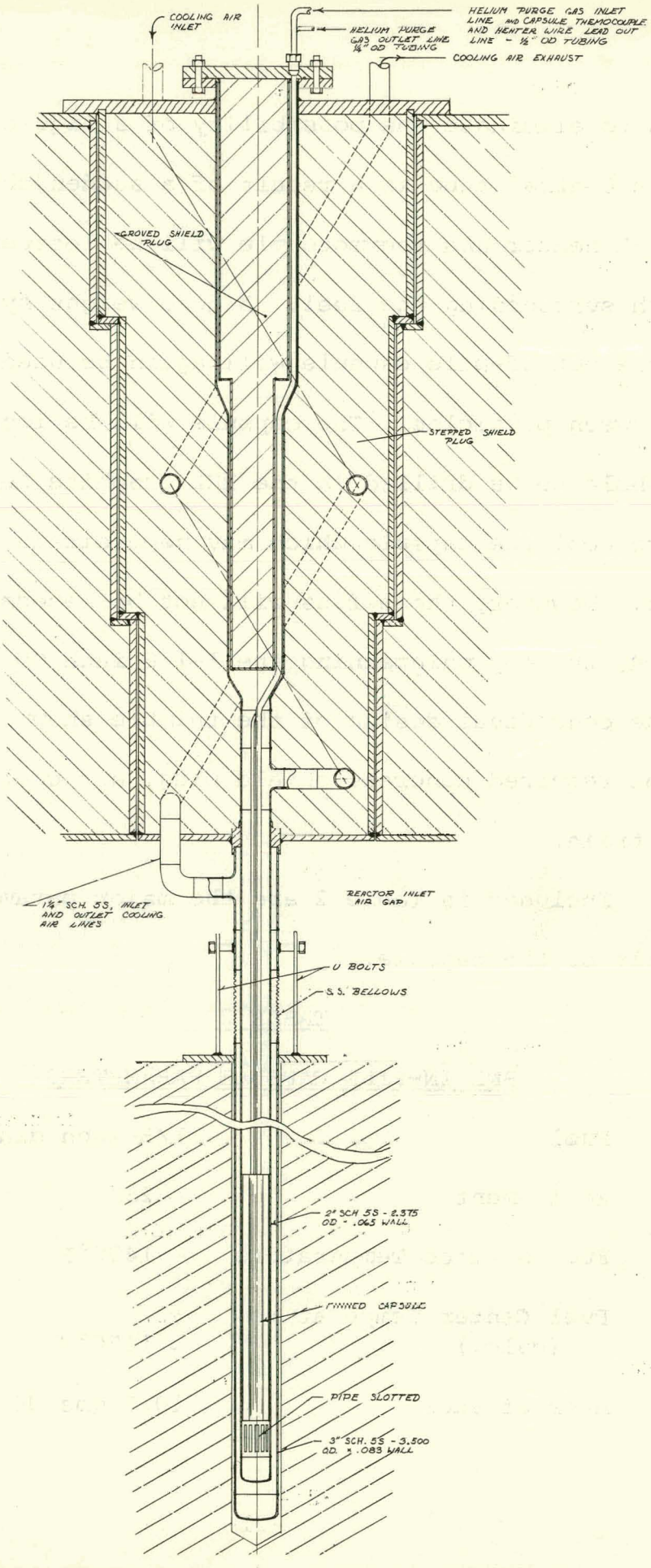

Figure 5. Conceptual design of BNL in-pile thimble.

Unperturbed Flux (thermal)	7.5×10^{12}
Fission Heat Generation	1,500 BTU/hr
Auxiliary Heat	2,500 BTU/hr
Design Heat Load	4,000 BTU/hr
Dead Weight Load	1 lb
Heat Sink	NaK
Coolant	Air
Heat Barrier	Helium
Capsule OD	1-1/8 inch
Material of Construction	type 316 SS

Availability of UC

The availability of test quantities of 1/8-inch uranium carbide in spherical form from commercial suppliers was investigated and the results are encouraging. The immediate purpose is to obtain the material as an "off the shelf" item without engaging in a fuel fabrication development program. This fuel will be used in the initial phase of the fuel development program, primarily in the out-of-pile capsules, in order to develop a set of specifications for the ultimate fuel system.

Six fuel suppliers were contacted and all except one have quoted on the material. As of this date 200 grams have been purchased and received from Vitro Laboratories.

The procedure with all fuel received from vendors is to perform both metallurgical and chemical analysis on a representa-

tive sample. This will provide a control for future out-of-pile and in-pile experiments.

The material received from Vitro appears to be very good with the exception of particle size and shape. A photograph of a representative grouping of the fuel particles is shown in Figure 6 and 7. The particle size ranges from 0.060 inches to 0.150 inches. The majority of the fuel particles were quite spherical but as can be seen there are some deviations from a perfect spherical condition. The variation in size is the result of a first attempt at fabrication of the spherical particles. The fabrication technique is a High Intensity Plasma Arc process.

Metallurgical examination of the fuel is very encouraging. As can be seen in Figures 8 and 9, there is no indication of any UC_2 needles, or any foreign material. The white areas in the grain boundaries are free uranium which is to be expected since the material is hypostoichiometric.

Capsule Program

The capsule program for evaluation of UC is given in Table 3. This includes both the out-of-pile and in-pile capsules. In all cases the heat sink will probably be NaK.

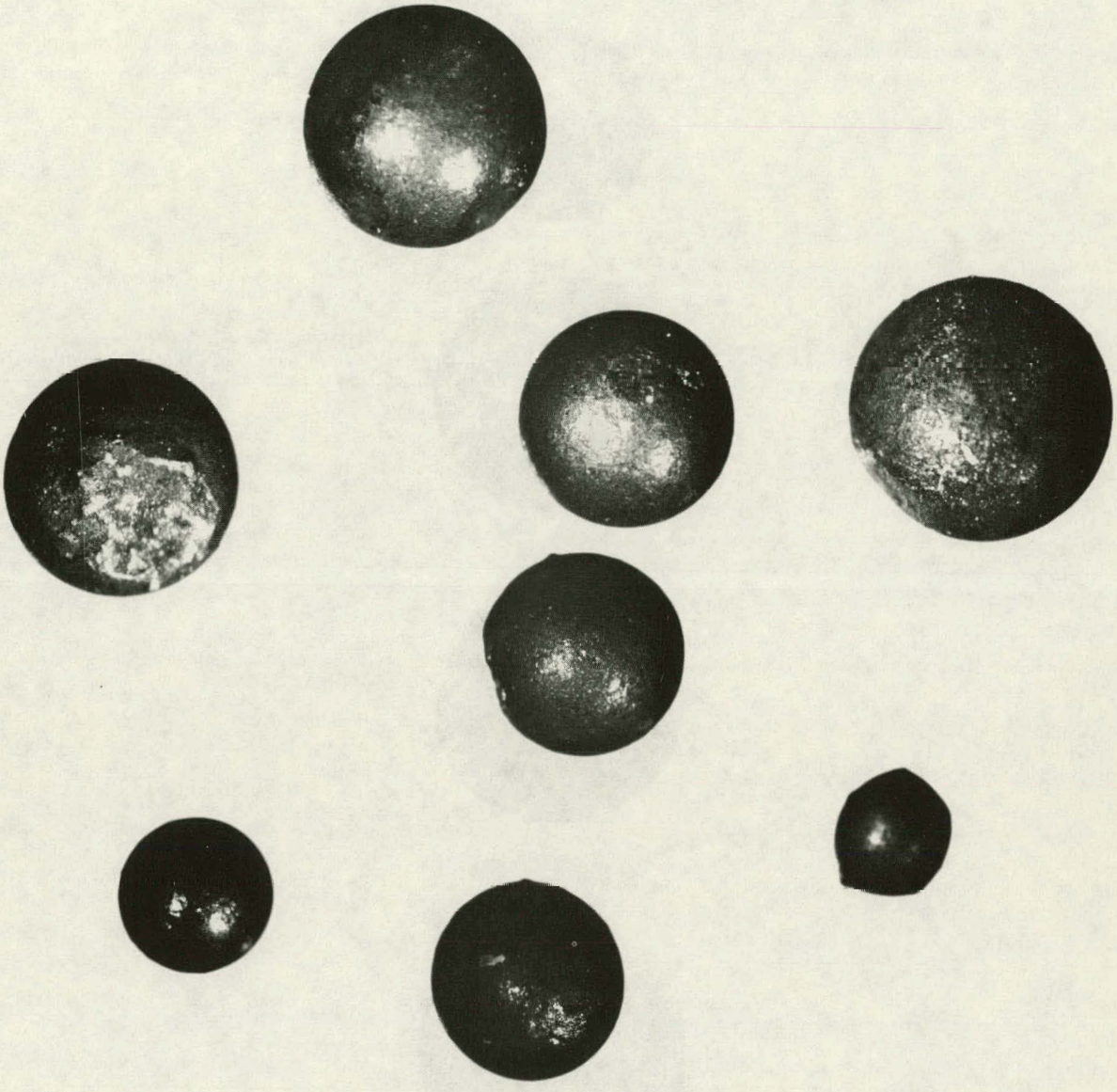

Figure 6. Uranium carbide spheres size range 0.060-0.150 inches diam.

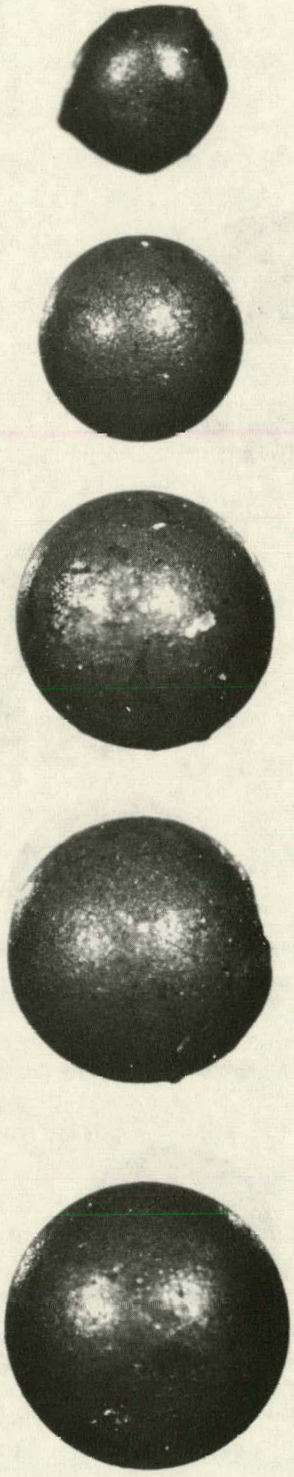

Figure 7. Uranium carbide spheres size range 0.060-0.150 inches diam.

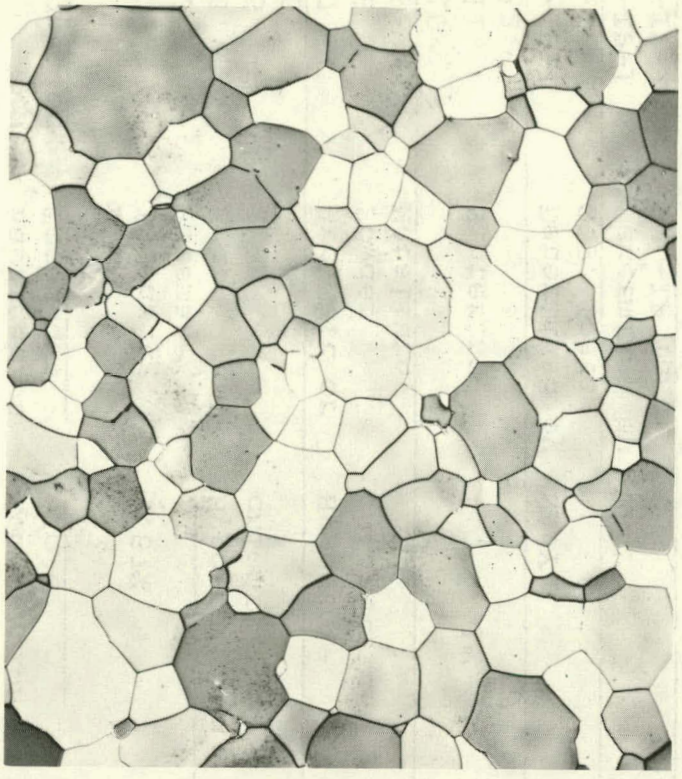

Figure 8. UC (4.7 w/o C). 150x. $HC_2H_3O_2$, HNO_3, H_2O etch.

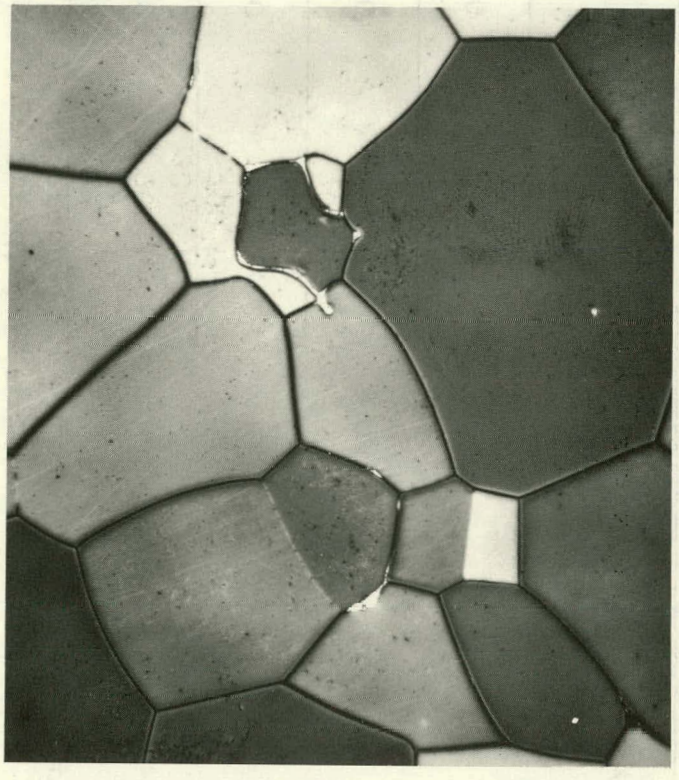

Figure 9. UC (4.7 w/o C). 500x. $HC_2H_3O_2$, HNO_3, H_2O etch.

TABLE 3

IN-PILE AND OUT-OF-PILE CAPSULE PROGRAM

Cap Designation	Fuel Fabrication Technique	Fuel Composition w/o C	Operating Temperature °F	Test Duration or Irradiation Period	Flux Level	Burnup A/o
OP-1	High		1450	700 hr		
OP-2	Intensity	4.67%	300-1450	700 hr	NA	
OP-3	Plasma		1450	3000 hr		
OP-4	Arc	Hypostoi-	1450	700 hr		
OP-5		chiometric	300-1450	700 hr	NA	
OP-6			1450	3000 hr		
OP-7	Arc Melt or	Hypostoi-	1450	700 hr		
OP-8	Powder	chiometric	300-1450	700 hr	NA	
OP-9	Metallurgy		1450	3000 hr		
OP-10			1450	700 hr		
OP-11	Sintering	$4.7 \pm .1\%$	300-1450	700 hr	NA	
OP-12			1450	3000 hr		
BNL-IP-1	Determined by	NAvY	1450	~ 5 mo	7.5×10^{12}	0.2%
BNL-IP-2	O.P. Tests		1450	~ 5 mo	7.5×10^{12}	0.2%
MTR-IP-1	Determined by	NAvY	1450	1 oper.cycle	2.5×10^{13}	0.35%
MTR-IP-2	BNL-IP Test		1450	~6 mo	2.5×10^{13}	5%

OP Out-of-Pile
IP In-Pile
NAvY Not Available Yet
NA Not Applicable

MECHANICAL DESIGN - RADIAL FLOW

The reactor vessel is 6.93 ft ID by 13.75 ft high with a 1¾ in. thick wall. It is designed for a pressure of 200 psig at 1200°F. The top head of the vessel is flanged and may be removed for maintenance of internal components. Contained within the reactor vessel are the core and blanket regions, coolant plenums, control rods, and support structures. See Figs. 10 and 11.

The vessel as well as all internal components in contact with sodium are of AISI Type 316 stainless steel.

Coolant enters the reactor vessel through 18 in. nozzles on both ends of a vertical 24 in. diameter pipe that runs through the reactor on the central axis. The central pipe is perforated with 1/16 in. wide by approximately 2 in. long slots in the region of the core. The slots account for approximately 50% of the surface area of the cylinder and will allow coolant to flow through the pipe wall while preventing the 1/8 in. diameter fuel particles from passing through. The coolant then flows radially through the annular core and leaves through the ½ in. thick cylindrical portion of the core vessel which is also perforated. The perforations in the central 24 in. pipe and the core vessel are spaced so that there is a slight downward component of flow through the fuel bed serving to hold the bed in a settled condition. After leaving the core the coolant flows downward through the blanket

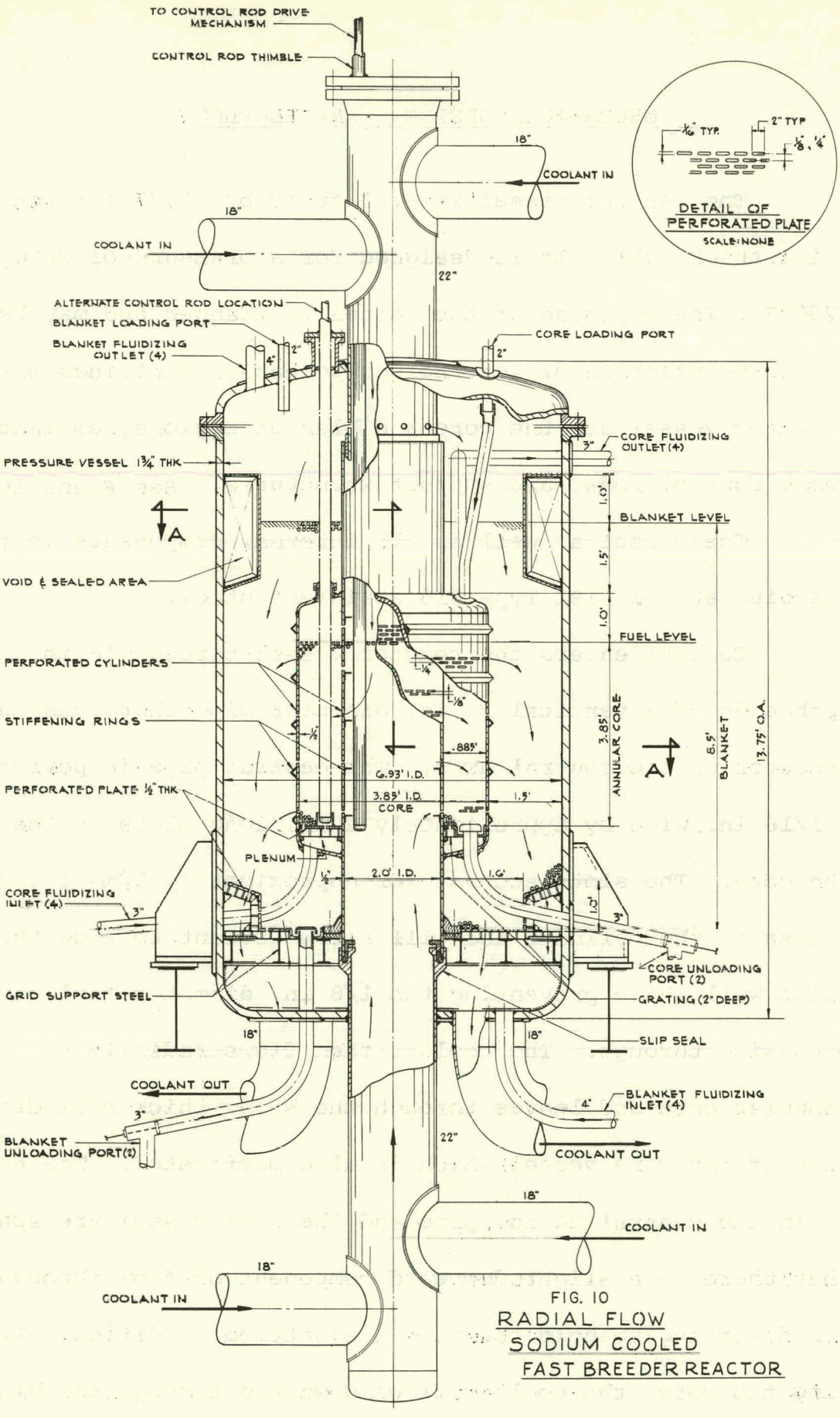

FIG. 10

RADIAL FLOW
SODIUM COOLED
FAST BREEDER REACTOR

VERTICAL SECTION-"B-B"

0 6" 1' 2' 3'

1" = 1'-0"

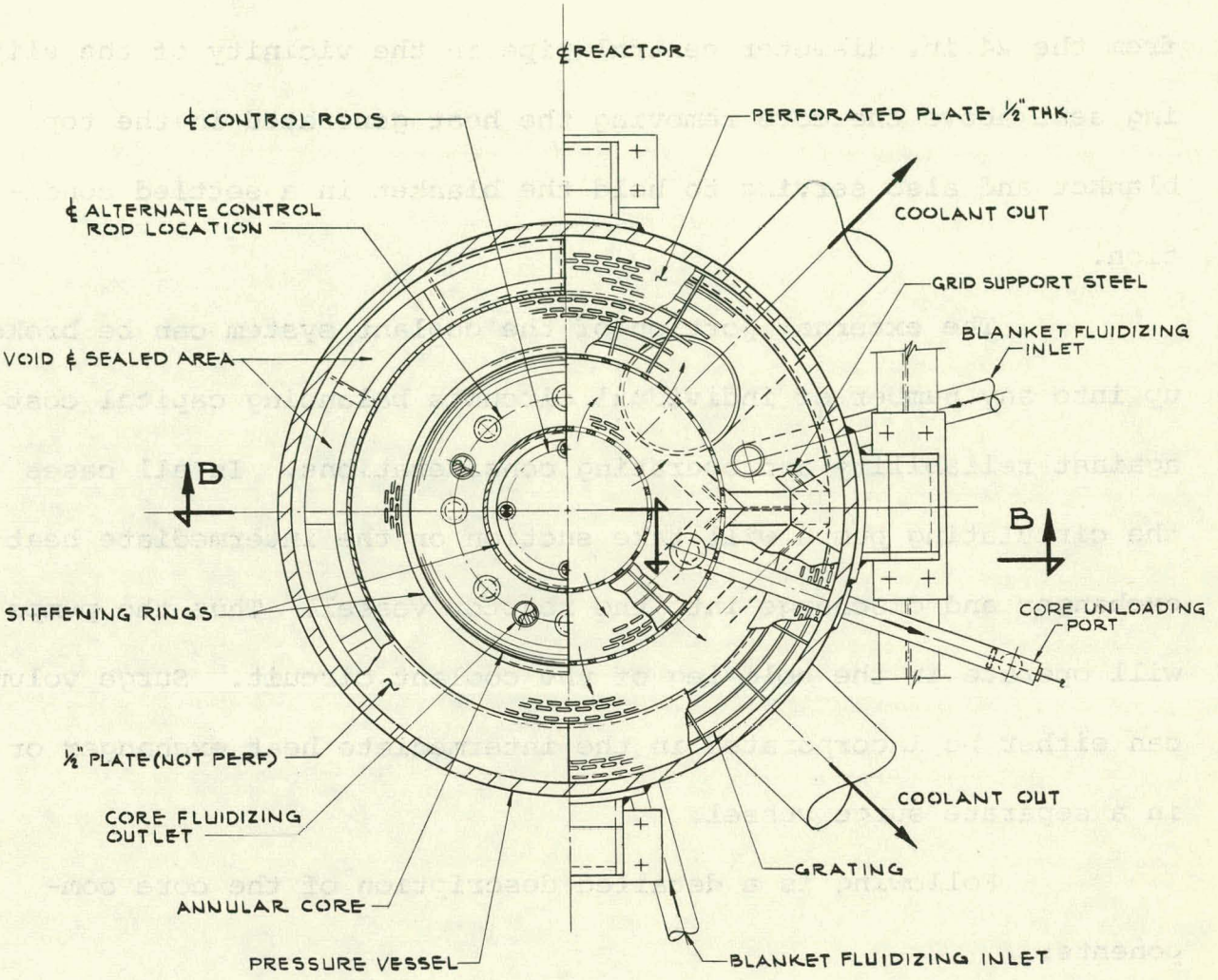

HORIZONTAL SECTION - "A-A"

0 6" 1' 2' 3'

1" = 1'-0"

FIG. 11

RADIAL FLOW SODIUM COOLED FAST BREEDER REACTOR

region, enters the lower plenum through the bottom perforated plate and leaves through four 18 in. diameter nozzles at the bottom of the reactor vessel. Some coolant is permitted to leak from the 24 in. diameter central pipe in the vicinity of the sliding seal above the core removing the heat generated in the top blanket and also serving to hold the blanket in a settled condition.

The external portion of the coolant system can be broken up into any number of individual circuits balancing capital cost against reliability and operating considerations. In all cases the circulating pumps will take suction on the intermediate heat exchanger and discharge into the reactor vessel. Thus the pumps will operate in the cold leg of the coolant circuit. Surge volume can either be incorporated in the intermediate heat exchanger or in a separate surge vessel.

Following is a detailed description of the core components:

1) Core Vessel and Central Coolant Pipe: The core vessel is 3.85 ft diameter by approximately 5 ft high with a 24 in. diameter pipe running vertically on the core central axis. Thus the fuel region is annular, 3.85 ft OD by 24 in. ID and 3.85 ft high. The extra height of the core vessel permits a 1 ft expansion of the fuel bed during fluidization.

The perforations in the core vessel and central pipe are

1/16 in. wide by approximately 2 in. long. If it proves too difficult to perforate ½ in. plate in this manner, the cylinder can be made up of ¼ in. plate with larger perforations with 1/8 in. perforated sheet attached to both sides. The 1/8 in. sheet would be punched with the desired perforations.

Stiffening rings are provided on both cylinders in order to prevent collapse under the bearing of the fuel and blanket pellets.

The core vessel is supported on the lower grid work by a section of the 24 in. central pipe. Sliding seals are incorporated in the upper and lower sections of the central pipe to accommodate differential expansions. Neither seal must be leak tight, in fact leakage is desired through the upper seal to permit coolant flow into the top blanket. Some effort is required to reduce leakage from the lower seal since cold inlet sodium is mixing with the hotter outlet sodium, however, absolute leak tightness is not a requirement. The slip seal shown here consists of a steel wool packing that can be compressed by an internal ring in the 24 in. central pipe. Access to this seal is through the flanged opening at the top of the central pipe.

The fuel pellets rest on a perforated plate at the bottom of the core vessel. The perforated plate rests on a grating support structure. A plenum below the support is fed by four 3 in. diameter fluidizing inlet lines. When the bed is

fluidized the sodium flows out through four 3 in. diameter pipes at the top of the core vessel. Both a fuel loading port and unloading port are provided. The unloading ports at the bottom support plate are furnished with traps that will not allow fuel to pass in the settled state, but will permit fluidized fuel to flow.

2) Blanket Region: Fertile material in the form of 1/8 in. pellets surround the core filling the space between the core vessel including the central pipe and the reactor vessel to a height 2.5 ft above the operating fuel level. Annular structures are attached to the reactor vessel in the top and bottom blanket regions. These form a void, the purpose of which is to provide an approximately constant cross section area throughout the blanket, permitting a better degree of fluidization.

Fluidizing sodium for the blanket enters through four 4 in. nozzles at the bottom of the reactor vessel, flows through the bottom plenum and distributes through the perforated plate into the blanket. This fluid leaves through four 4 in. nozzles at the top of the vessel. Again, a blanket loading port, and blanket unloading ports are provided. It should be noted that three sodium circuits communicate within the reactor vessel. The coolant stream, core fluidizing stream, and blanket fluidizing stream have in some cases common plenums, and in all cases can

communicate through perforated plates. However, only one fluid system is required to operate at any time and while one system is operating the others must be valved off in external piping to ensure the proper flow path.

3) Control Rods: Control rods are shown installed internally around the periphery of the 24 in. central pipe. An alternate location is shown within the fuel region. Either position is feasible and a final selection requires more detailed physics calculations. In either case the control rods would probably be 2 in. diameter boron steel rods in thimbles.

4) Support Structure: The core weight is approximately 18,000 lbs. This load is carried on the support structure at the bottom of the vessel through a portion of the 24 in. central pipe acting as a column. The blanket weight of approximately 150,000 lbs is also carried by the same support structure which consists of a continuous grating that supports the perforated plate. The grating in turn is supported on I-beam sections. A double row of I beams is provided to permit continuity of fluid in the lower plenum. The I beam grid work transmits the load to the vessel wall where the entire load of fuel, blanket, and vessel is carried by four external supports.

MECHANICAL DESIGN AXIAL FLOW

No additional mechanical design work was performed on the axial flow reactor, though heat transfer, fluid flow, physics and economics were done to accommodate the higher sodium outlet temperature. Characteristics of the axial flow reactor are given in the table of reactor characteristics. Figure 12 is a schematic of the reactor taken from BNL-5372. The height and diameter of the active core have increased to 7.29' x 4.37'. The major design features remain the same.

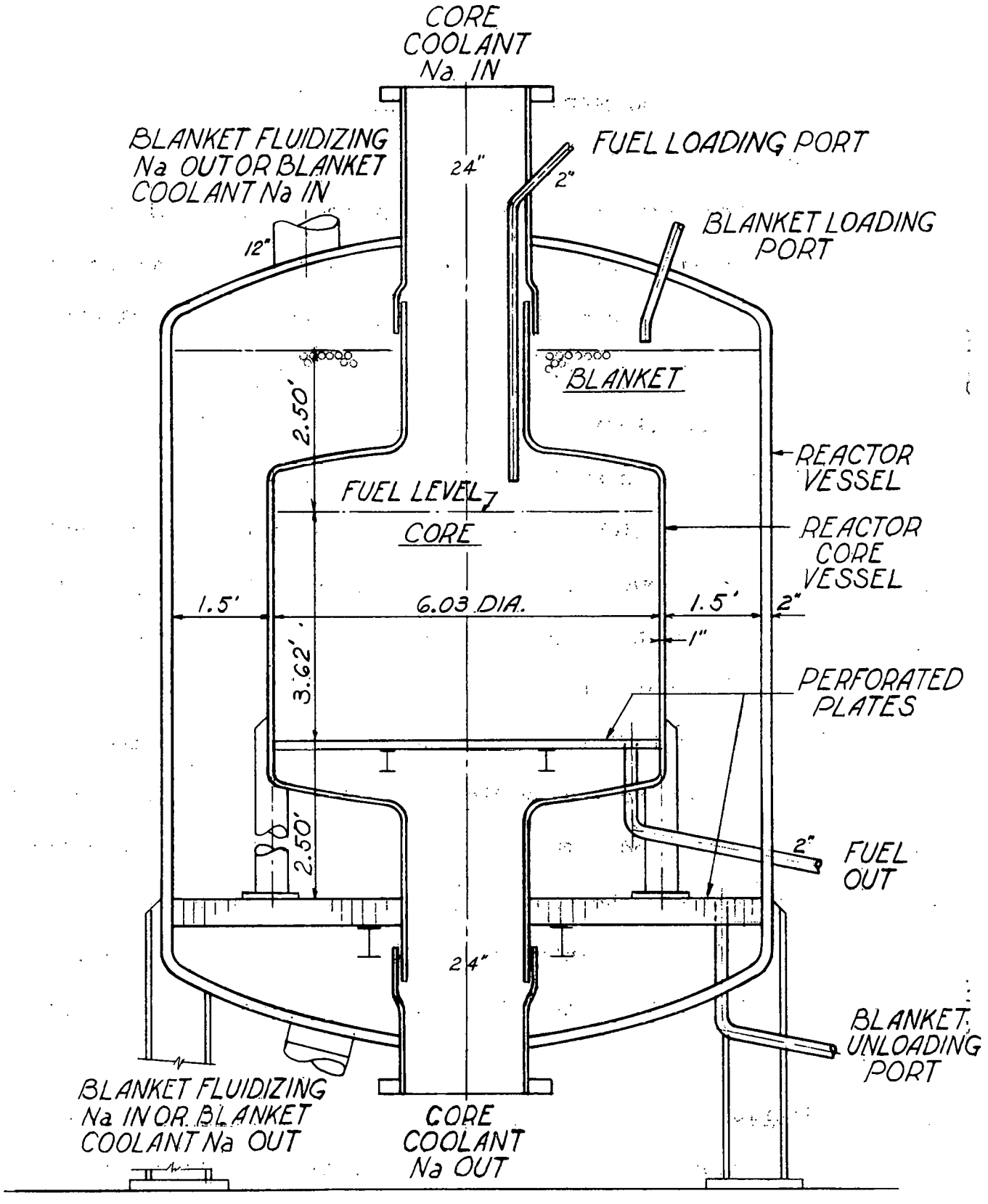

Figure 12.

SODIUM COOLED FAST BREEDER REACTOR
AXIAL FLOW TYPE

HEAT TRANSFER AND FLUID DYNAMICS

Introduction

The heat transfer results described on the following pages apply to solid fuel reactors cooled by forced convection of liquid sodium. The core consists of unclad spheres of fuel which form a settled particle bed. Sodium fills the spaces between particles, and when flowing, permits high heat transfer rates. The large heat transfer surface present in a particle bed also assists in achieving high power density. The fact that the fuel can be fluidized allows the entire core to be periodically "homogenized" and then settled for another period of operation, permitting a uniform fuel burnup with time.

Two coolant flow concepts have been considered in detail. The first, has downward sodium flow, parallel to the axis of a cylindrical settled bed. The second flow concept has coolant flow radially outward from the axis of a cylindrical settled bed. In this case the coolant is introduced to the fuel region by first flowing through a hollow pipe which penetrates the center of the cylindrical core.

Design Criteria

In order to utilize the high thermal efficiency of the most modern steam plants a reactor coolant outlet temperature of 1200°F was prescribed. Previous work as reported in reference

(1) differs only in that the coolant outlet temperature is 1050°F.

The survey of potential fuel types was extended to include metal alloys of the Uranium-Plutonium-Molybdenum system. A literature search was also performed to obtain more recent data on the physical properties of the fuel types considered. An allowable tensile stress equal to 10,000 psi for uranium carbide was employed in thermal stress calculations. This allowable stress sets the largest permissable particle diameter for a fixed peak heat generation rate. Therefore, in order to achieve a lowering in fuel volume, weight, and capital charges, for conditions of fixed thermal power output, it is desired to reduce the diameter of the fuel particle. A reduction in fuel particle diameter, however, increases the core pressure drop and hence pumping power. The particle diameter given in this section for each reactor is an optimum value producing minimal annual cost for pumping and fuel inventory.

A review of pressure drop correlations for liquid flow in packed or settled beds was made. A parametric survey was then made for the range of particle diameters, flow rate, viscosity and porosity of interest in this study. The correlation selected for use[2] generally predicts a higher pressure drop than other expressions. Conservative values of calculated pressure drop are considered desirable at this time in view of the un-

certainties in particle uniformity, roughness and sphericity. Radial and axial power peaking factors were used for each reactor configuration in conjunction with physics data. A hot channel factor equal to 1.17 was employed in all reactor calculations. The hot channel factor is the same value used in the Atomic International study[3], and is intended to reflect the influence of deviations in particle geometry on local coolant flow and bulk temperature rise. Also, a heat transfer factor equal to 1.25 was applied to the fuel temperature rise in the region of over-all power peaking in order to compensate for variations in heat flux around the surface of any single particle. This factor is the same as used in the ORNL pebble bed study[4]. The particle maximum thermal stress was determined using this factor together with overall power peaking factors.

Results and Discussion

The pertinent heat transfer data are presented in the Table of Reactor Characteristics. The advantages of the radial flow core relative to the axial flow core have become even greater at 1200°F than in the previous designs with a sodium outlet temperature equal to 1050°F. From the standpoint of thermal and hydraulic considerations, oxide or carbide fuel could be used successfully. Uranium carbide because of its greater thermal conductivity permits twice the power density relative to oxide fuel,

and therefore half the fuel inventory.

For a thermal power of 824 MW, the radial flow carbide reactor requires 32.6 ft^3 of which 40% is sodium. The design flow of 1.42×10^7 lbs/hr removes the heat in changing temperature from 550°F to 1200°F. The hot channel factor of 1.17 and the axial flux peaking factor of 1.40 combine to produce a hot channel maximum sodium temperature of 1615°F.

This maximum temperature occurs at the outlet. Methods of reducing this temperature were not considered in order to preserve the basis of comparison among the different reactors studied. The precise effects of interchannel mixing have not been determined and because of the small particle diameter, a reduction of maximum sodium and fuel temperature is anticipated with no change in other parameters. In the event that further study reveals that interchannel mixing is not sufficient to produce more uniform coolant outlet temperatures, this still may be brought about. If the core tank diameter is varied smoothly from a maximum at the end planes to a minimum at the core mid-plane, then together with the cylindrical central coolant pipe it becomes possible to design the core for isothermal coolant outlet temperature. The resulting reactor would possess isothermal coolant outlet temperature and through periodic fluidization, would yield a uniform fuel burnup.

SETTLED BED STABILITY

Calculations in the physics section of this report on the effect of bed settling on reactivity, indicate as expected a positive effect. The magnitude of this effect is dependent on the core size, the larger cores being less sensitive than the small cores. Though these calculations are extremely rough and must be refined by using two dimensional codes, it is believed that the trend is correct based on the assumptions made. Prompt criticality for these reactors is obtained at a k_{excess} of $\sim$ 0.004, which is the delayed neutron fraction. For the worst case, <u>total</u> bed settling in a vertical direction, a change in void fractions of 1.5%, 1.8% and 4.6% respectively for the radial carbide, radial oxide and axial carbide cores amounts to one dollar's worth of reactivity. It is important to point out, however, that in the radial flow cores where the vertical effect is strongest the flow pressures in a horizontal direction greatly exceed the gravitational forces in the vertical direction and that bed compaction, if it does occur, will be in an outward direction. Physics calculations for this occurrence have not been undertaken at this time though it is expected that the reactivity effect will be considerably smaller than for the vertical compaction case.

In any event, unless as a result of refined calculations the magnitude of the effect is reduced to a very small value, it is considered imperative that the bed be brought to a stable degree of

compaction. With this requirement in mind, rough experiments were performed with a bed of 0.09-inch spherical lead particles to gain some insight into the matter of reproducibility of bed compaction by various methods. The methods included impact vibration of bed, mechanical vibration of bed, pulsed fluidizing flow, slow fluidizing shut off, and rapid fluidizing shut off. The last three methods require manipulation of the fluidizing stream. The results indicated for any one method or combination of methods that the compaction was reproducible although each different method gave a different void fraction. The range of void fractions for all the methods was between 33% and 36%. In practical terms the object is to obtain bed compaction such that the coolant stream during power operation produces no significant effect. In addition, compaction should be such that vibration due to nearby equipment and earth or building tremor due to earthquake, explosion or the dropping of heavy equipment should not produce compaction in excess of one half the percentage capable of producing prompt criticality. It should be noted that nuclear calculations were carried out for 40% void fraction. Actually, as a result of the compaction experiments void fraction will be 33% or less and physics work will be redone at these new values.

An essential part of the development program for this fuel cycle system is an experimental effort whose objective is to verify a stable state of compaction. An ideal close packed array of

uniform size spheres results in a void fraction of approximately 26%. A uniform packing of this type would be obtainable only by "hand" assembly of the array. A mechanical method must be found which will allow realistic packing densities to be obtained in a practical system.

One such method which suggests itself is ultrasonics. The ultrasonic generator or transducer can be located outside the reactor biological shield. The energy would then be transmitted through a rod directly into the bed of spherical particles. If void fractions less than 33% can be obtained by this method further packing by normal means, i.e. fluid flow, low frequency vibration or earth tremor would be highly improbable.

REACTOR PHYSICS

Introduction

The principal method of analysis used for these fast reactors was multi-group, one dimensional diffusion theory. The diffusion equation was solved numerically by the use of the Atomics International AIM-6 code[1]. This code utilizes a library of microscopic cross section data, and has provision for a concentration search on one or two elements, as well as for an extensive edit of output data. Modifications of the AIM-6[2] code have been made to allow neutrons from a given group to scatter to six successive lower groups instead of the maximum of five permitted by the original FORTRAN dimension statements, to allow storage of the microscopic cross section data library on binary tape rather than on binary cards, and to allow AIM-6 to be run on the IBM-704 computer which was available for BNL use at the time this work was begun.

The microscopic cross sections used in these calculations were the 11 group set of Loewenstein and Okrent[3]. For use in burnup calculations, cross sections for Pu^{242} and Pu^{241} were taken to be the same as for Pu^{240} and Pu^{239}, respectively, except for the values of ν for Pu^{239} and Pu^{241} which were taken to be in the same ratio as the values for thermal fission. Average absorption cross sections per fission product pair for use in burnup calcu-

lations were based on the work of Greebler, Hurwitz and Storm[4]. The group structure over which the averaging was performed was taken to be the same as that of the other elements.

Method of Calculation

The volume fractions of the various materials were established from the reactor design. From these volume fractions and the densities of the various materials (Table 4), the average isotopic concentrations of the various isotopes were computed for each region.

TABLE 4

Material Densities Used In Settled Bed Fast Reactor Calculations

Material	Density, gm/cm^3
Steel	7.78
Sodium	0.832
UO_2-PuO_2	10.0
UC-PuC	12.8

Using these concentrations as input to the AIM-6 code, a search was performed, in cylindrical geometry, for the ratio of U^{238}/Pu^{239} concentrations which gave a value of $k_{eff} = 1.01$. The initial reactor parameters are all based on this as a reference value for k_{eff}. There is, however, no particular significance in this choice of a nominal one percent excess reactivity, and it seems quite feasible in the fuel cycle for these reactors not to require more than one dollar in excess reactivity because of burnup considerations.

An initial excess reactivity less than the present 1% would correspond to an increase in the U^{238}/Pu^{239} ratio, and a gain in the breeding ratio.

A neutron balance for the reactor, as well as the initial reactor parameters and the spectrum and power distribution were obtained from the AIM-6 data edit. The partial breeding ratio obtained by this method is defined as the ratio of non-fission capture in U^{238} in a given region to the total absorption in Pu^{239} in the reactor. The total breeding ratio is the sum of the partial breeding ratios for all regions. The breeding ratio obtained from the neutron balance is the initial value, as are the values listed for the other parameters unless otherwise noted.

Changes in reactivity and fuel isotopic composition with time were investigated using a one group model. The fuel cycle studied was one where the reactor operates at constant power for a specified period. After each burnup period (one month intevals in this case) sufficient Pu^{239} is added to/or fuel removed from the core so that the effects of fuel burnup and fission product build-up are overcome, and reactivity is restored to just the value at the beginning of core life time. Some approximations were made in the course of this calculation. First the 11 group cross sections were averaged over the initial core spectrum to give average one group cross sections. These average cross sections were then used throughout the calculation and changes that would actually occur

in the spectrum with time were neglected. One group equations were then written to compute the average flux in the core (for a specified power level), reactivity and isotopic concentrations as a function of time. The isotope concentration equations were written as difference equations to facilitate computation. The time interval of one month used in this calculation was sufficiently small not to introduce a noticable error in the solution of the differential equations. These equations were then solved using the IBM-610 computer to obtain the monthly changes in reactivity and core composition. Because of the simple model used,, it was not possible to include changes due to the buildup of plutonium in the blanket. It is to be expected that plutonium will be built up, preferentially on the inner edge of the blanket, close to the core, where it will have the greatest influence on reactivity. Power and reactivity pertubbations due to the non-uniform spatial buildup of plutonium may be minimized by fluidizing the blanket also at times when the core is fluidized for fuel changes. This will permit mixing and a consequent uniform distribution of plutonium in the blanket. Changes in reactivity, and breeding ratios with time, and the rate at which fissionable material is consumed or bred, depend, of course, on the power level at which the reactor is operated and the fuel management schedule that is followed. The results reported here apply only to the specific methods used.

Effective Delayed Neutron Fraction, Prompt Neutron Lifetime and Absorber Worth

The effective delayed neutron fraction was computed from the expression:

$$\beta_{eff} = \frac{\sum_{m=1}^{NFI} \left[\int_{vol} \left(\sum_{j=1}^{NOG} \beta^m \nu_j^m \Sigma_{fj}^m(r) \varphi_j(r) \right) \left(\sum_{j=1}^{NOG} x_j^{1\,m} \varphi_j^+(r) \right) dV \right]}{\sum_{m=1}^{NFI} \left[\int_{vol} \left(\sum_{j=1}^{NOG} \nu_j^m \Sigma_{fj}^m(r) \varphi_j(r) \right) \left(\sum_{j=1}^{NOG} x_j^m \varphi_j^+(r) \right) dV \right]}$$

where

m = index of fissionable isotope

NFI = total number of fissionable isotopes

NOG = number of groups

j = group index

ν_j^m = total number of neutrons per fission in group j for isotope m

$\Sigma_{fj}^m(r)$ = macroscopic fission cross section in group j for isotope m at radius r

$\phi_j(r)$ = flux in group j at radius r

β^m = delayed neutron fraction for isotope m

x_j^m = the fraction of fission neutrons from isotope m born into group j

$$\left[\sum_{j=1}^{NOG} x_j = 1.0 \right]$$

x_j^{1m} = the fraction of delayed fission neutrons from isotope m born into group j

$$\left[\sum_{j=1}^{NOG} x_j^{1m} = 1.0 \right]$$

$\phi_j^+(r)$ = adjoint flux in group j at radius r

The fluxes and adjoints were computed and punched on cards by AIM-6. The delayed neutron data was taken from ANL-5800[5] and the effective delayed neutron fraction for the reactor was evaluated on the IBM-7090 using a program written in FORTRAN. The prompt neutron lifetime was evaluated from

$$l_p = \frac{\int_{vol} \sum_{j=1}^{NOG} \phi_j^+(r) \; \Sigma_{aj}(r) \; \phi_j(r) \; dV}{\sum_{m=1}^{NFI} \left[\int_{vol} \left(\sum_{j=1}^{NOG} \nu_j^m \; \Sigma_{fj}^m(r) \; \phi_j(r) \right) \left(\sum_{j=1}^{NOG} x_j^m \; \phi_j^+(r) \; dV \right) \right]}$$

where $\Sigma_{aj} = \left(\frac{\overline{1}}{v}\right)$ = the average of the reciprocal of the velocity of a neutron in group j. In the calculation of both the effective delayed neutron fraction and the prompt neutron lifetime, the spatial integration was carried out over the whole reactor. The reactivity worth of absorber as a function of radial position was evaluated on the IBM-7090 from an expression identical with the one for the prompt neutron lifetime. In this case, however Σ_{aj} was the macroscopic absorption cross section of boron containing isotopes in their natural isotopic abundance. The microscopic boron absorption cross sections were taken from the work of Yiftah, Okrent and Moldauer[6]. The 16 group cross sections in their work were reduced to the 11 group set actually used by weighting over the core spectrum in each of the reactors studied. The isotopic concentration of boron used (0.11×10^{24} atoms/cm^3) was

taken to correspond to the concentration of boron in B_4C. The integration of the numerator was performed over a unit area at each radial position.

The results then apply to a reactivity change produced by an annulus of absorbing material at radius r having thickness (1/r) cm and extending the entire height of the core. To the accuracy with which linear perturbation theory applies, an annulus at radius r having a thickness Δr cm will produce a change in reactivity $r \cdot \Delta r$ times as large as that produced by an annulus of thickness 1/r. Similarly, a ring of annular segments that subtend an angle of less than 360° may be expected to produce a change in reactivity approximately given by the change produced by a complete annulus times the fraction of the annulus that they occupy. The reactivity worth of B^{10} in this reactor will be approximately 5 times as much as that for natural boron, per gram.

Discussion of Results

The neutron flux spectrum for the radial flow design with carbide fuel is shown in Figure 13 . The radial power distribution is shown in Figure 14. The relatively low ratio of the maximum to average radial power generation rate is due to the absence of the central position of the core which would ordinarily have the highest power generation rate. The median flux energy as a function of position in the reactor, and median fission energy as a

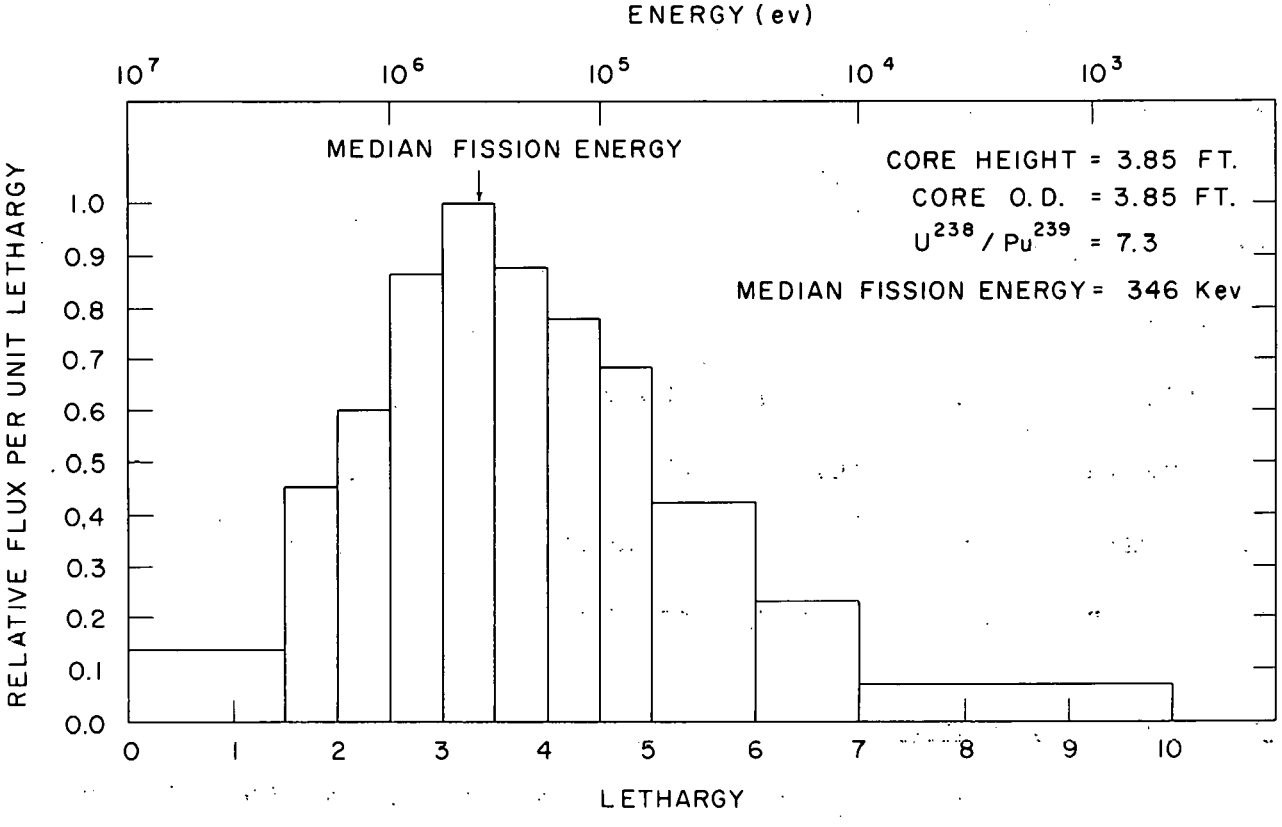

Figure 13. Neutron flux spectrum - radial flow carbide fuel.

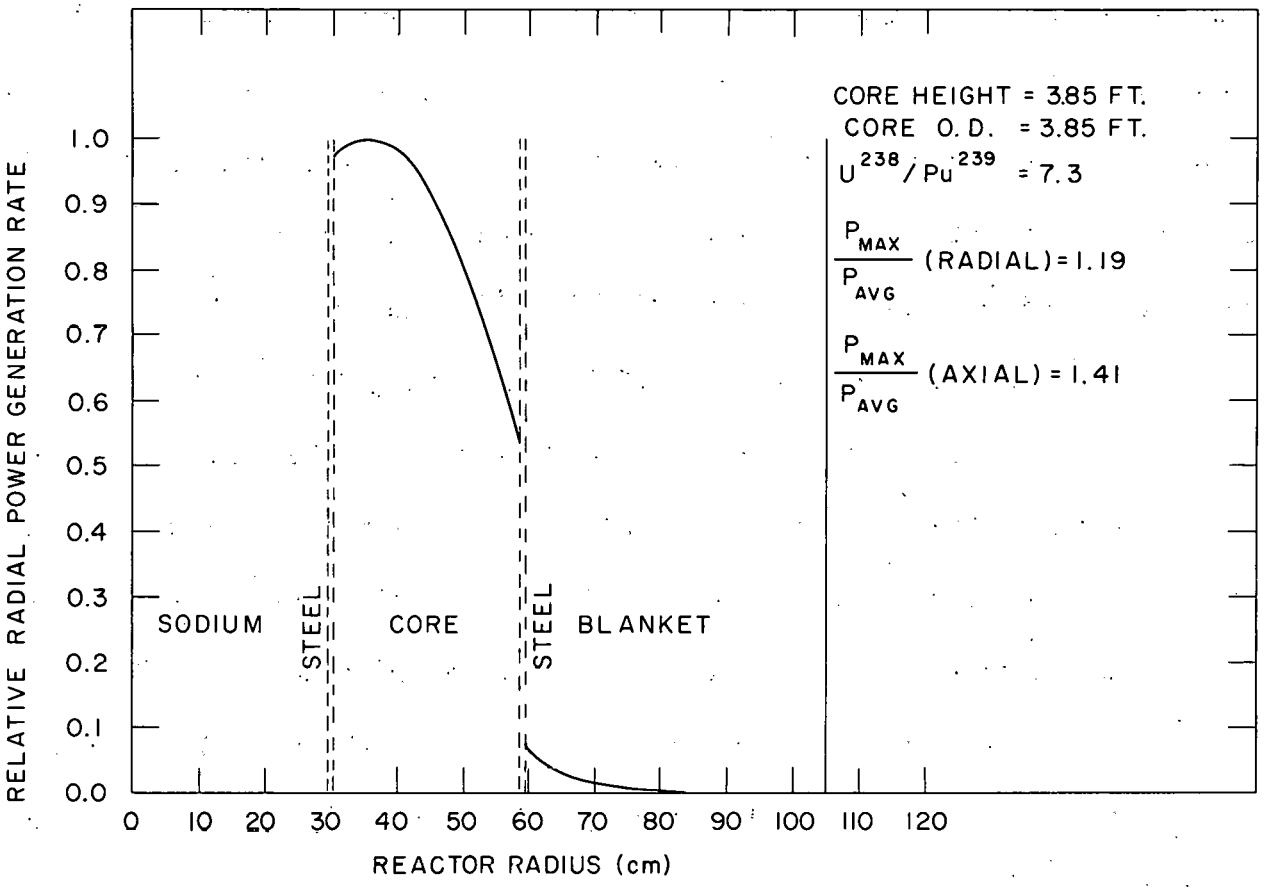

Figure 14. Radial power distribution - radial flow carbide fuel.

function of position in the core are shown in Figure 15. The spectra in the coolant pipe and blanket are softer than in the core, and since the core is a relatively thin annulus, the spectrum varies somewhat from one position to another in the core. The neutron balance for this reactor is presented in Table 5. The large neutron leakage for this design consists principally of leakage from the central coolant pipe. The parameters of interest for the carbide fueled radial flow design are shown in Table 6**. The initial fuel loading for one percent excess reactivity is 812 kg Pu^{239}. This corresponds to a U^{238}/Pu^{239} ratio of 7.34. The partial breeding ratio in the core is 0.7612 initially and the partial breeding ratio in the blanket is 0.7299 for a total of 1.4912. The fact that the partial breeding ratio in the core is less than unity means that fuel must be added to the core periodically in order to maintain reactivity. Over a 24-month period* a total of 206 kg Pu^{339} must be added to the core to compensate for the burnup of Pu^{239} and accumulation of fission products. Changes in core com-

---

* Burnup studies for all designs were based on a reactor power of 815 MW(t). Since the actual thermal power output varies from one design to another, the monthly burnup period is a nominal one, and must be reduced in the ratio of 815 to the actual power in order to obtain the true time.

** Table of Reactor Characteristics.

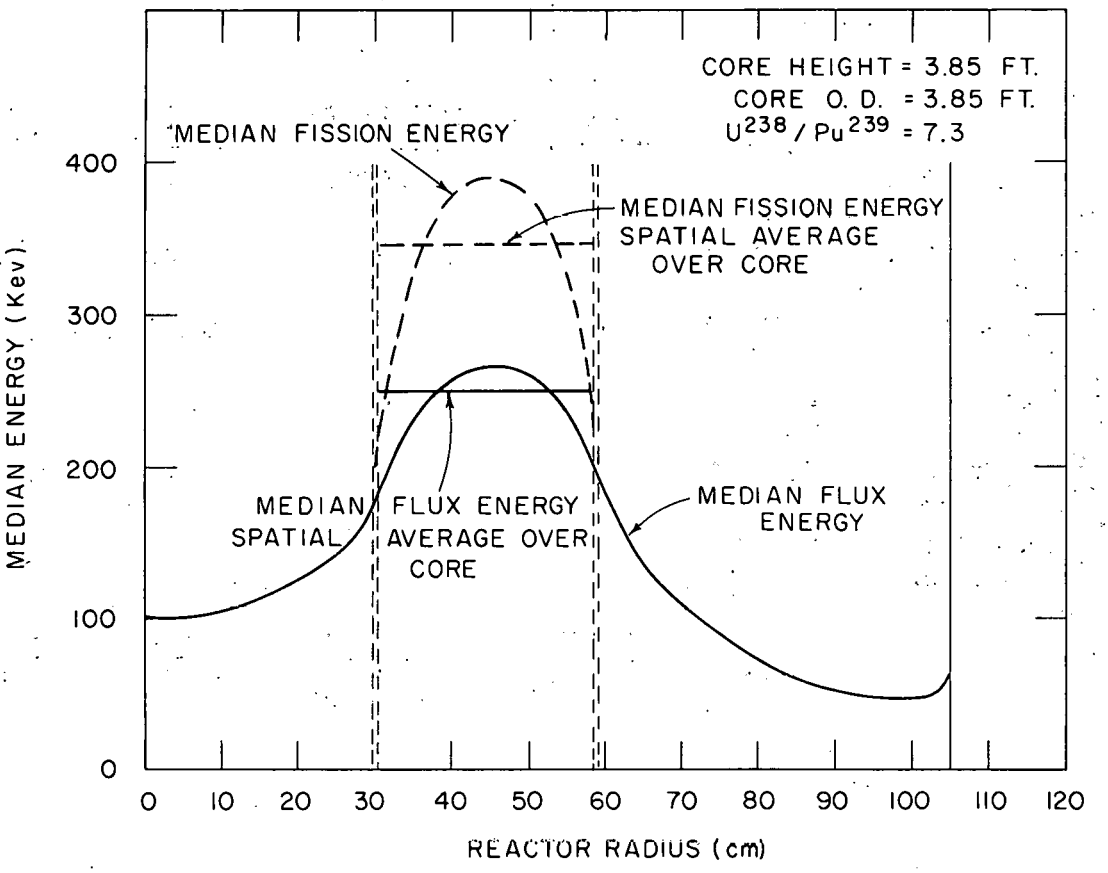

Figure 15. Median fission energy and median flux energy as a function of position - radial flow carbide fuel.

TABLE 5

NEUTRON BALANCE FOR RADIAL FLOW
FAST REACTOR WITH CARBIDE FUEL
(U^{238}/Pu^{239} = 7.34; k_{eff} = 1.01)

	Core	Coolant Channel	Structure	Blanket	Total
Steel Absorption	-	-	0.0020	-	0.0020
Sodium Absorption	0.0007	0.0010	-	0.0006	0.0023
U^{238} Capture	0.2580	-	-	0.2473	0.5053
U^{238} Fission	0.0635	-	-	0.0157	0.0792
Pu^{239} Capture	0.0636	-	-	-	0.0636
Pu^{239} Fission	0.2753	-	-	-	0.2753
Leakage	-	-	-	-	0.0723
	0.6611	0.0010	0.0020	0.2636	1.0000

position also cause a decrease in the breeding ratio as the reactor operates. The average decrease in k_{eff} per month is ~ 0.005, but this does not take into account contributions to reactivity from Pu^{239} bred in the blanket. The true average decrease in k_{eff} per month would be expected to be closer to 0.004. Since the effective delayed neutron fraction for this reactor is ~ 0.004, it seems possible to operate this reactor on refueling intervals of approximately one month and still not need an excess reactivity greater than one dollar at the beginning of a fueling interval to allow for burnup effects. Doubling time for these designs have been estimated using a time-averaged partial breeding ratio in the core, and the initial value of the partial breeding ratio in the blanket. It has also been assumed that all of the breeding is done in one reactor. Under these conditions, the time required for each reactor to produce a net gain of Pu^{239} equal to the original loading of Pu^{239} was estimated. The time required to produce a net gain (amount bred minus amount consumed) of plutonium (all isotopes) equal to the original fuel loading was also estimated. The difference is due almost entirely to Pu^{240}. The concentration of isotopes higher than this is negligible. If it is assumed that there exists a set of similar reactors, so that as plutonium is bred it may immediately be used to partially fuel another reactor, and itself begin to be used for breeding, the doubling time becomes significantly shorter.

The neutron flux spectrum for the oxide fueled radial flow reactor is shown in Figure 16. This core has a larger volume and lower fuel density than the carbide fueled radial flow design, and a comparison of the two designs shows that the oxide fueled core has a "softer" spectrum and a lower median fission energy. The variation of spectrum with position in the core is illustrated by Figure 17. Since the core annulus is thicker than for the carbide fueled design, and the spectrum in the core is closer to that in the coolant pipe and blanket, it does not vary as much from one position to another as it does in the carbide fueled design. The power distribution for this design is shown in Figure 18, and the neutron balance in Table 7. The reactor parameters are listed in Table 6. The initial fuel loading for this design is 1096 kg Pu^{239}, and the U^{238}/Pu^{239} ratio is 7.68. The volume of the oxide fueled radial flow core is much larger than that of the carbide fueled core, and though the fuel density is less, and the Pu^{239} constitutes a smaller fraction of the total fuel, the core loading still is larger. The spectrum is "softer" in the oxide core than in the carbide, and the capture-to-fission ratio in Pu^{239} has increased from 0.2309 to 0.2622. While the total breeding ratio is smaller than for the carbide design (1.414 compared with 1.491), the partial breeding ratio in the core is larger (0.846 vs 0.761). This core breeding ratio results in an average monthly decrease in k_{eff} of $\sim$ 0.003, which is less than the effect-

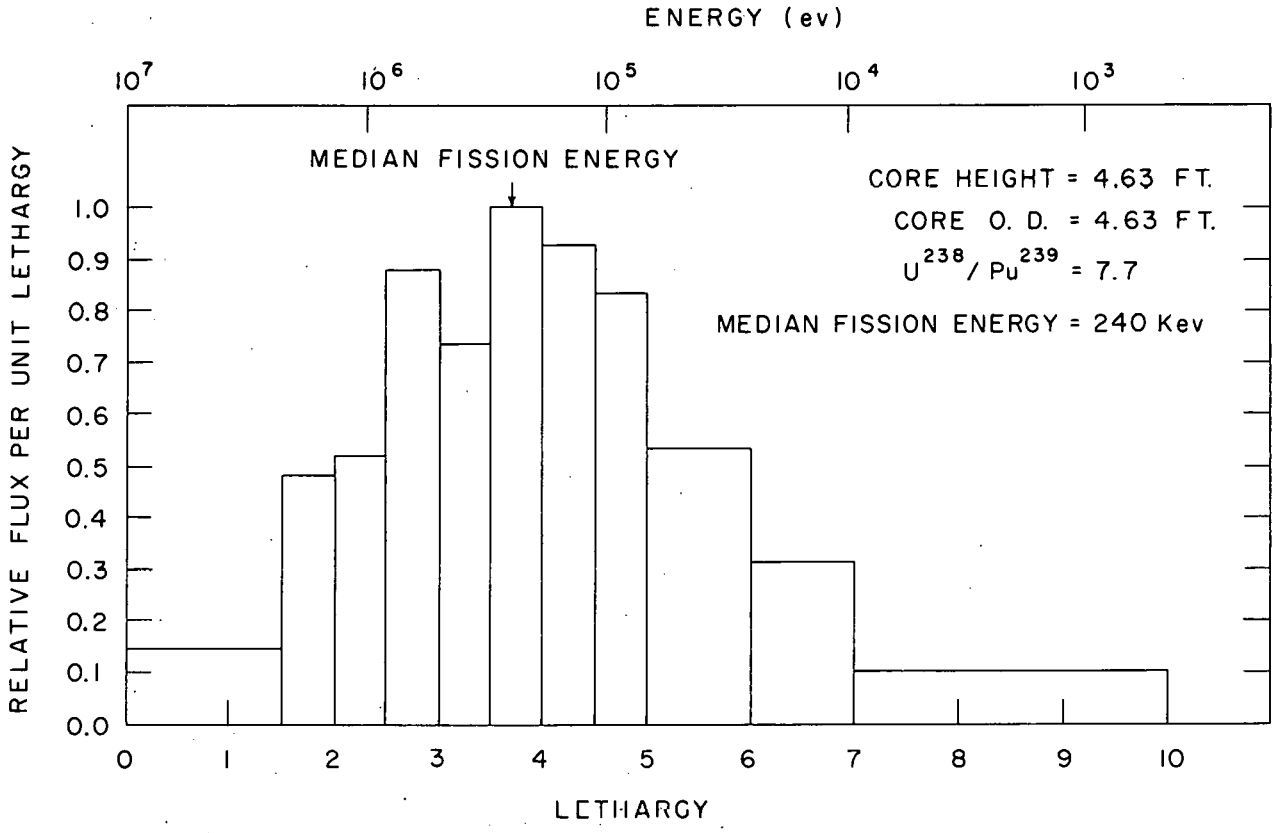

Figure 16. Neutron flux spectrum - radial flow oxide fuel.

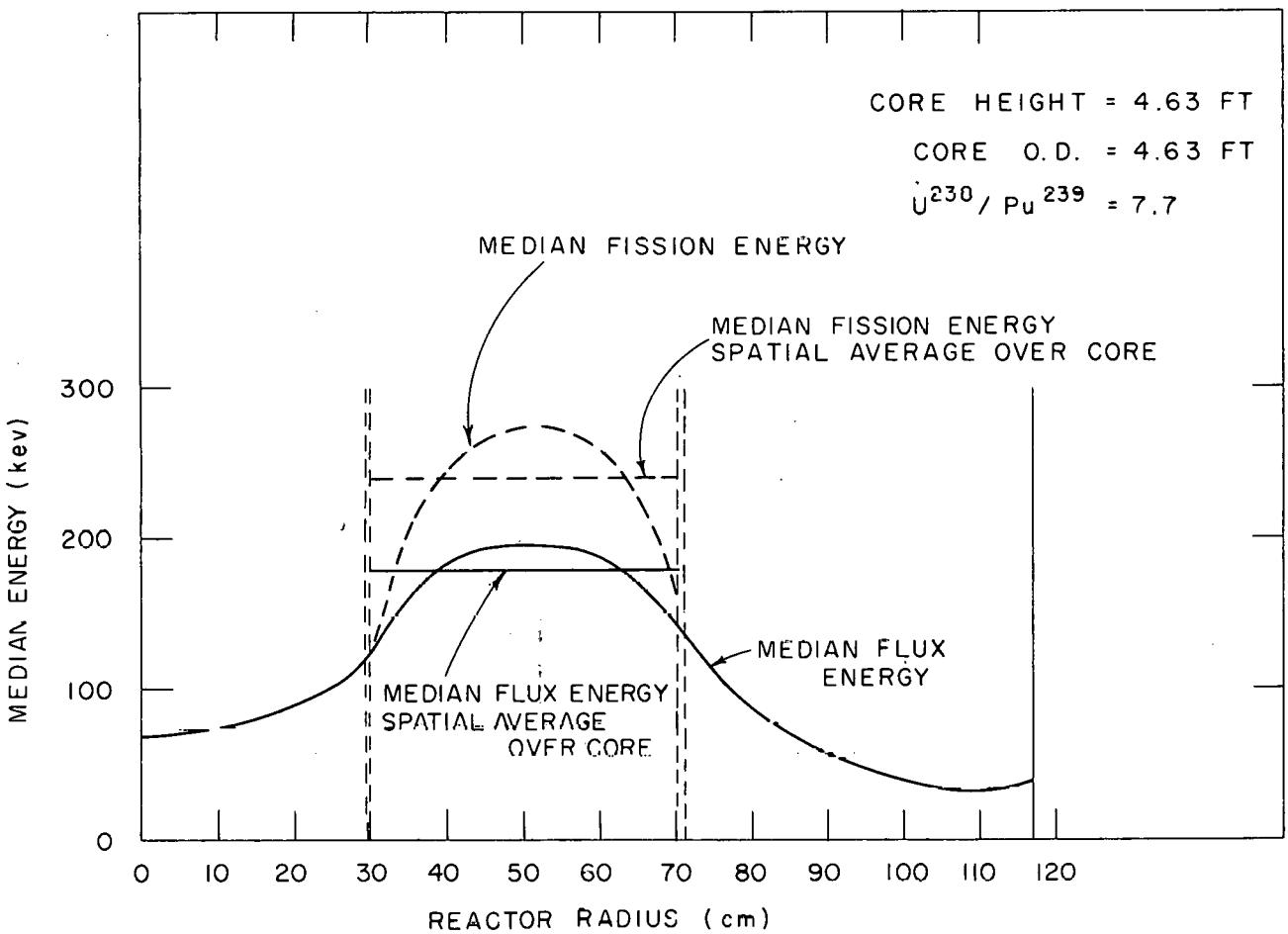

Figure 17. Median fission energy and median flux energy as a function of position - radial flow oxide fuel.

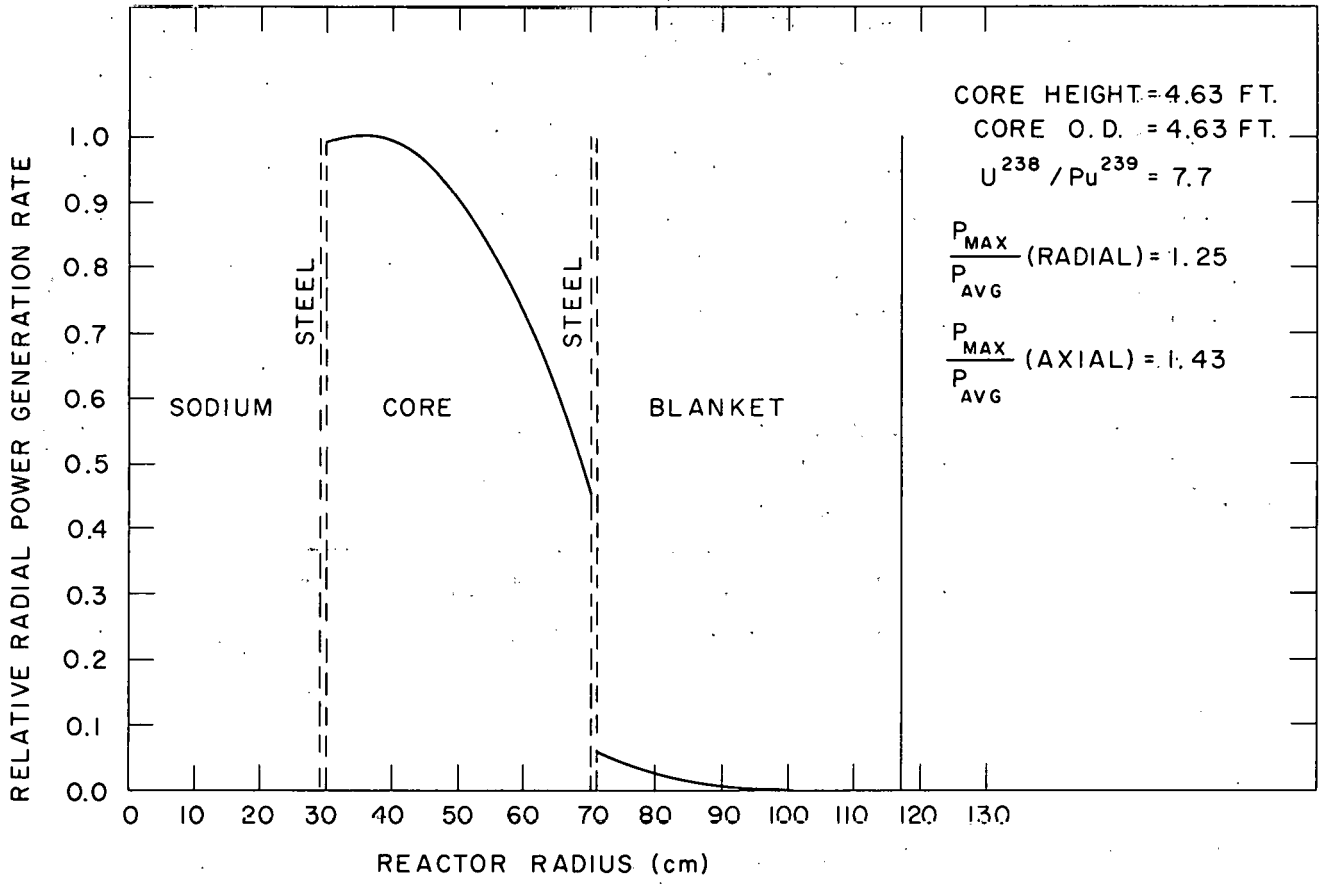

Figure 18. Radial power distribution - radial flow oxide fuel.

TABLE 7

NEUTRON BALANCE FOR RADIAL FLOW
FAST REACTOR WITH OXIDE FUEL
(U^{238}/Pu^{239} = 7.7; k_{eff} = 1.01)

	Core	Coolant Channel	Structure	Blanket	Total
Steel Absorption	-	-	0.0020	-	0.0020
Sodium Absorption	0.0010	0.0011	-	0.0007	0.0028
U^{238} Capture	0.2972	-	-	0.2000	0.4972
U^{238} Fission	0.0628	-	-	0.0124	0.0752
Pu^{239} Capture	0.0729	-	-	-	0.0729
Pu^{239} Fission	0.2785	-	-	-	0.2785
Leakage	-	-	-	-	0.0714
	0.7124	0.0011	0.0020	0.2131	1.0000

ive delayed neutron fraction for this design. Additions of fuel at intervals of approximately one month in order to maintain reactivity are therefore feasible in this core also without introducing more than one dollar of excess reactivity at the beginning of the interval.

The neutron flux spectrum for the axial flow design with carbide fuel is shown in Figure 19 . The spectrum is harder than that for the oxide fueled design, but not so hard as that for the smaller radial flow carbide fueled reactor. The radial power distribution is shown in Figure 20. The larger value of the ratio of the maximum radial power generation rate to the average radial power generation rate is due to the larger core diameter. The ratio of the maximum axial power generation rate to the average axial power generation rate is 1.343. This is not only smaller than the value for the oxide radial flow core which is taller, but also less than the value for the carbide radial flow design which is shorter. There are two reasons for this, both related to the axial blankets. One reason is that while the radial and axial flow designs both have a distance of 2.5 ft between the top of the core and the top of the top blanket, the axial flow design also has this blanket thickness on the bottom, whereas the radial flow design has only 2.17 ft on the bottom. The other difference is that in the axial flow design the core coolant inlet, a two foot diameter pipe, is directly over the core and hence forms part of the top and

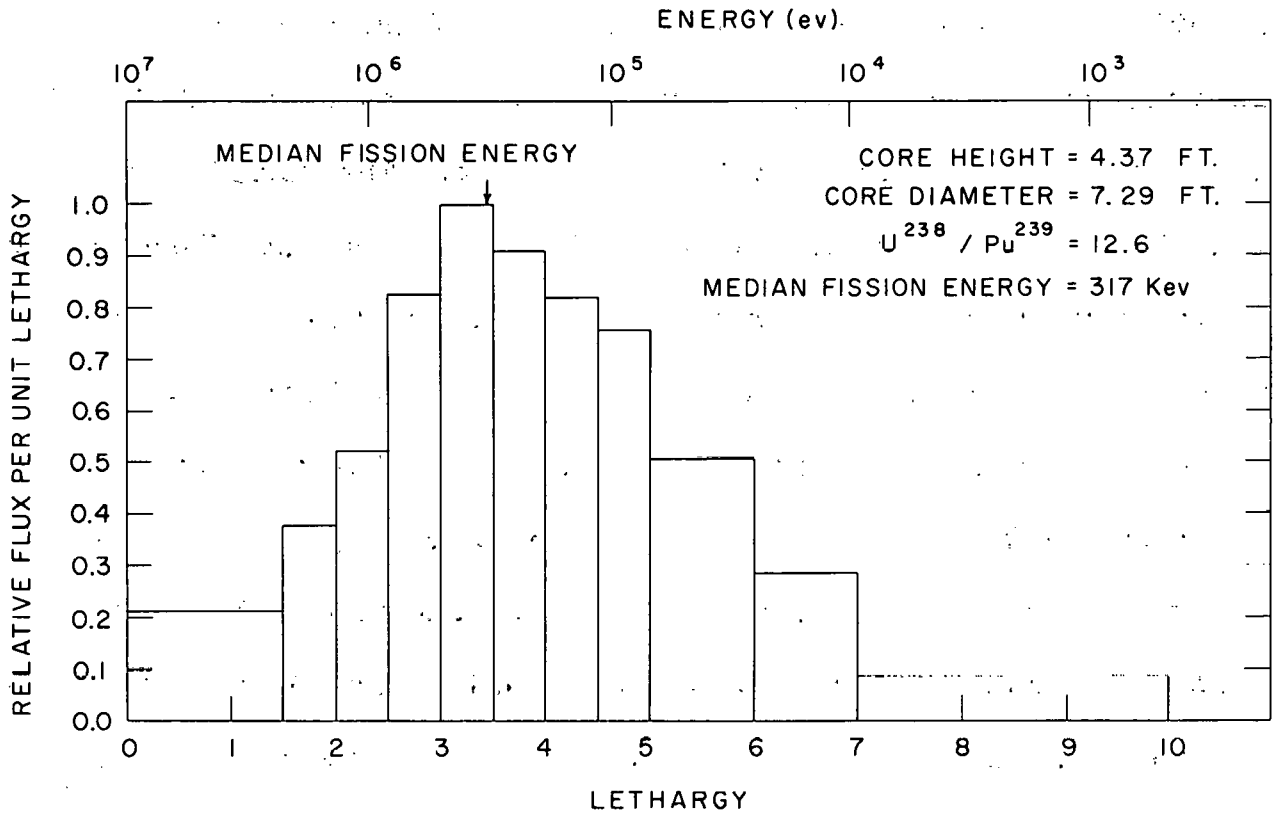

Figure 19. Neutron flux spectrum - axial flow carbide fuel.

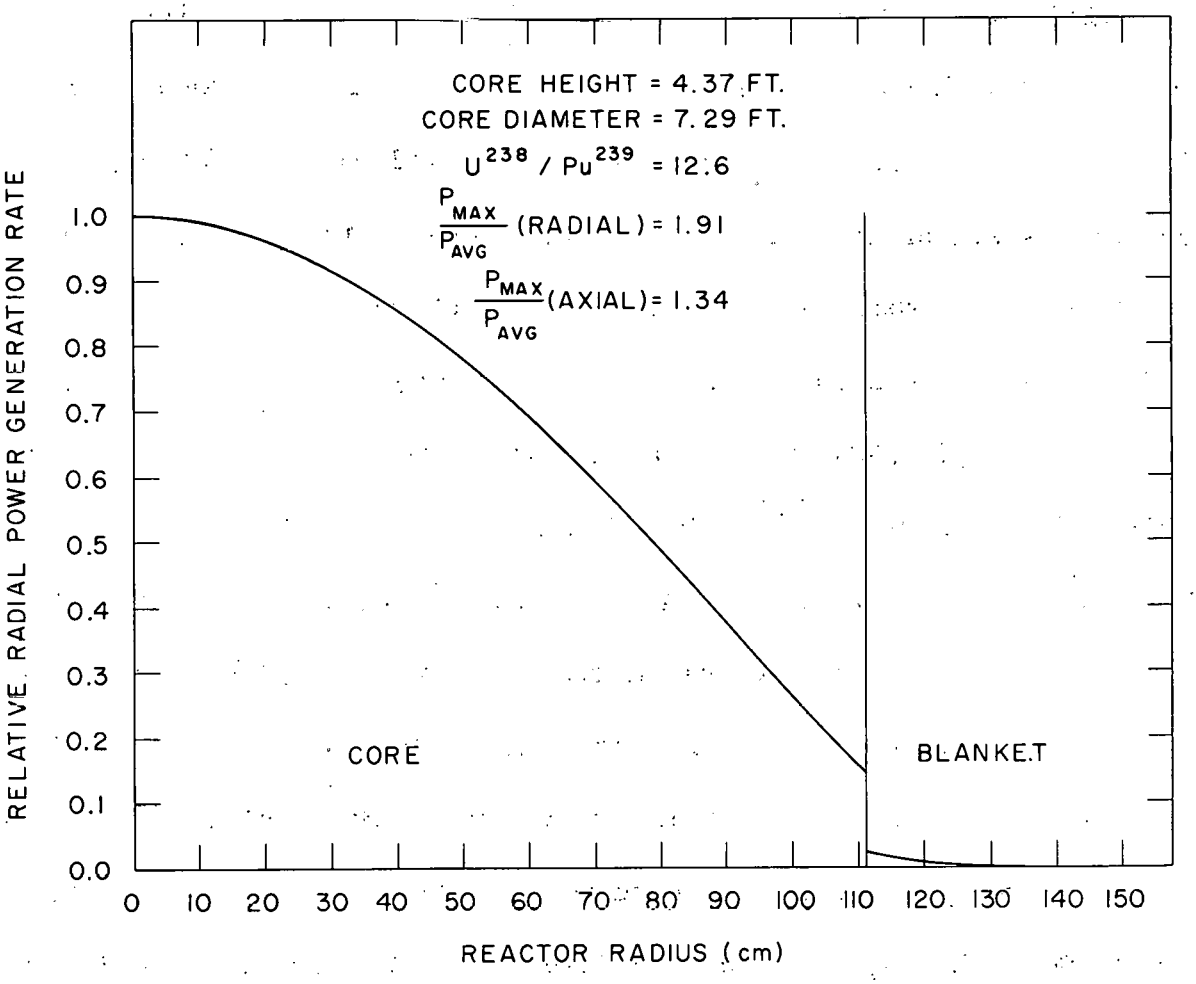

Figure 20. Radial power distribution - axial flow carbide fuel.

bottom reflector. In a one dimensional analysis this was homogenized with the blanket proper. This sodium absorbs neutrons less strongly than the blanket proper, and since it is a good scatterer returns many of them to the core. The lower ratio of the axial maximum power generation rate to average power generation rate of the axial flow design is due to the fact that the reflector on the bottom is thicker, and has more effective average properties.

The neutron balance for the axial flow carbide fueled reactor is shown in Table 8 . The leakage from this large core is very small as would be expected. The initial parameters are given in Table 6 . The plutonium is a small fraction of the fuel (U^{238}/Pu^{239} = 12.57), but because the core is so large, the fuel loading is 2783 kg Pu^{239}. The initial value of the breeding ratio for this reactor is 1.683. A particular feature of this design is that the partial breeding ratio in the core is 1.374 - greater than unity. As a result the reactivity and plutonium content of the core will increase with time. Time dependent reactor parameters for this design (Table 9) were obtained using a 45 month rather than a 24 month cycle, and a different method of fuel management. After the first month of operation, the reactivity will have increased by an amount Δk_{eff} equal to 0.00133 and there will be a net gain (amount bred minus amount consumed) of 9.38 kg of Pu^{239} and 5.07 kg of higher isotopes of plutonium. A fraction of the core mass (plutonium + uranium + fission products) sufficient to restore

TABLE 8

NEUTRON BALANCE FOR AXIAL FLOW FAST REACTOR WITH CARBIDE FUEL

(U^{238}/Pu^{239} = 12.6; k_{eff} = 1.01)

	Core	Structure	Blanket	Total
Steel Absorption	-	0.0003	-	0.0003
Sodium Absorption	0.0012	-	0.0002	0.0014
U^{238} Capture	0.4615	-	0.1036	0.5651
U^{238} Fission	0.0817	-	0.0049	0.0866
Pu^{239} Capture	0.0676	-	-	0.0676
Pu^{239} Fission	0.2682	-	-	0.2682
Leakage	-	-	-	0.0108
	0.8802	0.0003	0.1087	1.0000

TABLE 9

TIME DEPENDANT REACTOR PARAMETERS FOR THE AXIAL FLOW FAST REACTOR WITH CARBIDE FUEL

	1st Month	After 45th Month	Average
Core Breeding Ratio	1.374	1.152	1.263
Δk_{eff}/month	+0.00133	+0.00100	+0.00057
Net Gain in Pu^{239}/month in Core, kg	9.38	3.97	6.49
Net Gain in Total Pu/month in Core, kg	14.44	8.81	11.45
Pu^{239} Removed from Core/ month, kg	31.67	8.77	18.26
Total Pu Removed from Core/ month, kg	31.73	9.52	18.88
Percent of Core Mass Remaining*	98.9	72.0	81.4

*Core Mass = Plutonium + Uranium + Fission Products

k_{eff} to its original value is then removed. Since the material removed must be homogeneous, it includes, for the first month, 31.67 kg of Pu^{239}, 0.06 kg of the higher plutonium isotopes, and such amounts of fission products and U^{238} as to leave 98.9 percent of the original core mass remaining. After the second month of operation, k_{eff} will have increased by a smaller amount, and the net gain in Pu^{239} will be smaller. As a result, a smaller amount of material must be removed from the core to restore the reactivity to its initial value. The size of these changes over a 45 month period, and the average over a 45 month period are shown in Table 9 . These changes refer to the core only, and do not include changes in the contribution that the blanket makes toward maintaining reactivity. The total amount of material removed from the core over a 45 month period will result in a reduction in the core height of approximately 14.7 inches.

REACTOR CONTROL

Reactor control has been studied using first order linear perturbation theory, and the results for the three reactor designs are shown in Figures 21, 22, and 23 in the form of curves for reactivity worth of boron absorber per unit area as a function of position. Since the two radial flow designs are smaller than the axial flow, the reactivity worth per unit area of an absorber is greater at a given radius. In the axial flow design the value of an absorber is largest near the center of the core as would be expected. In the two radial flow designs, the effect of placing an absorber in the coolant pipe is even larger than placing it in the core. The importance, particularly of the high energy group is less in the coolant pipe than in the core, and the higher energy group fluxes are lower. However, the low energy group fluxes in the coolant pipe are even larger than in the core (a softer spectrum) and the importance of these low energy groups is no less in the coolant pipe than in the core. In addition, the absorption cross section of boron increases rapidly with decrease in spectrum so that it is a more effective absorber in the coolant pipe than it is even in the core.

Sodium Coefficient of Reactivity

It was first pointed out by Nims and Zweifel[9] that the sodium reactivity coefficient may be positive for some fast reactor

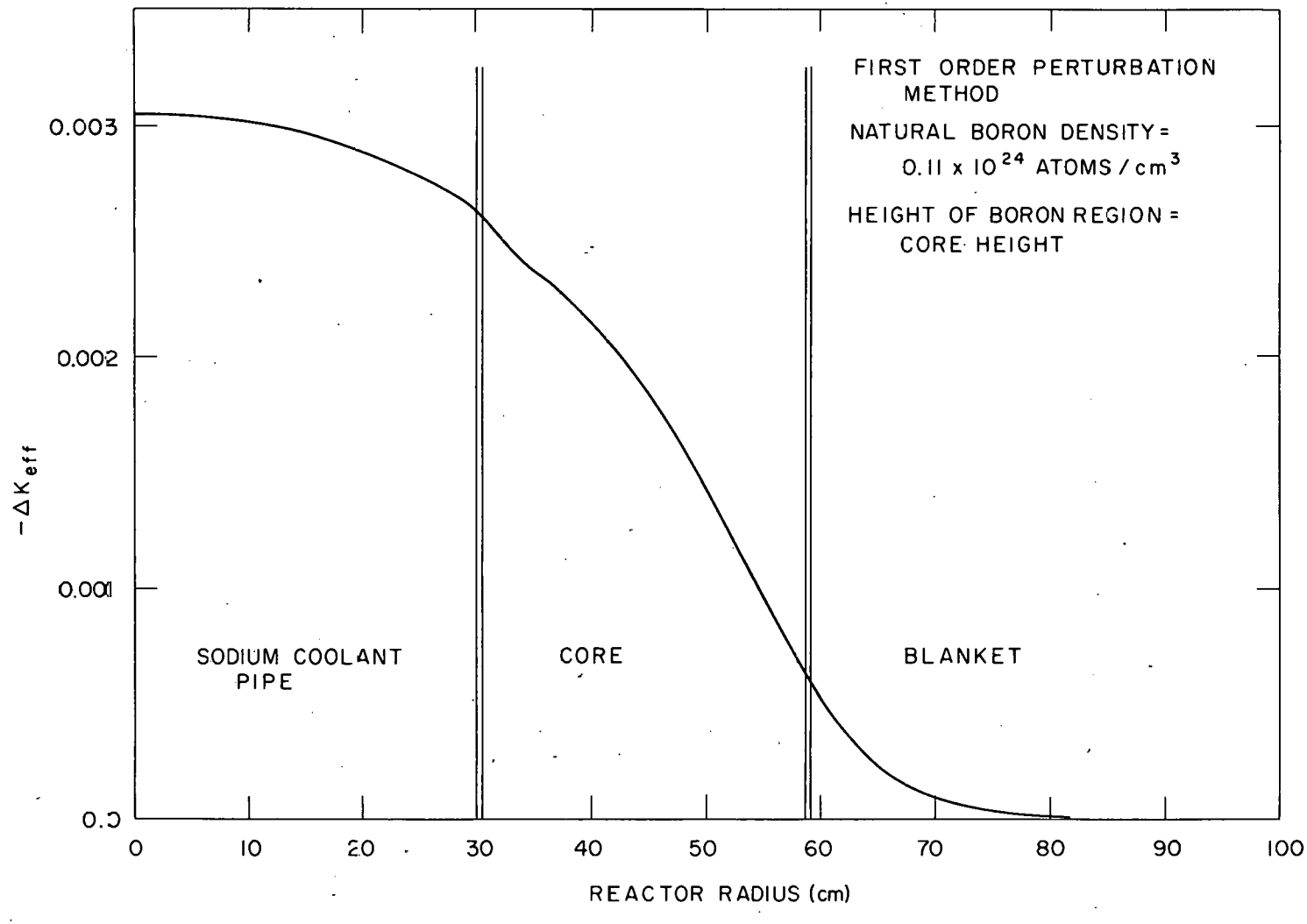

Figure 21. Reactivity worth of natural boron absorber per unit area as a function of position - radial flow carbide fuel.

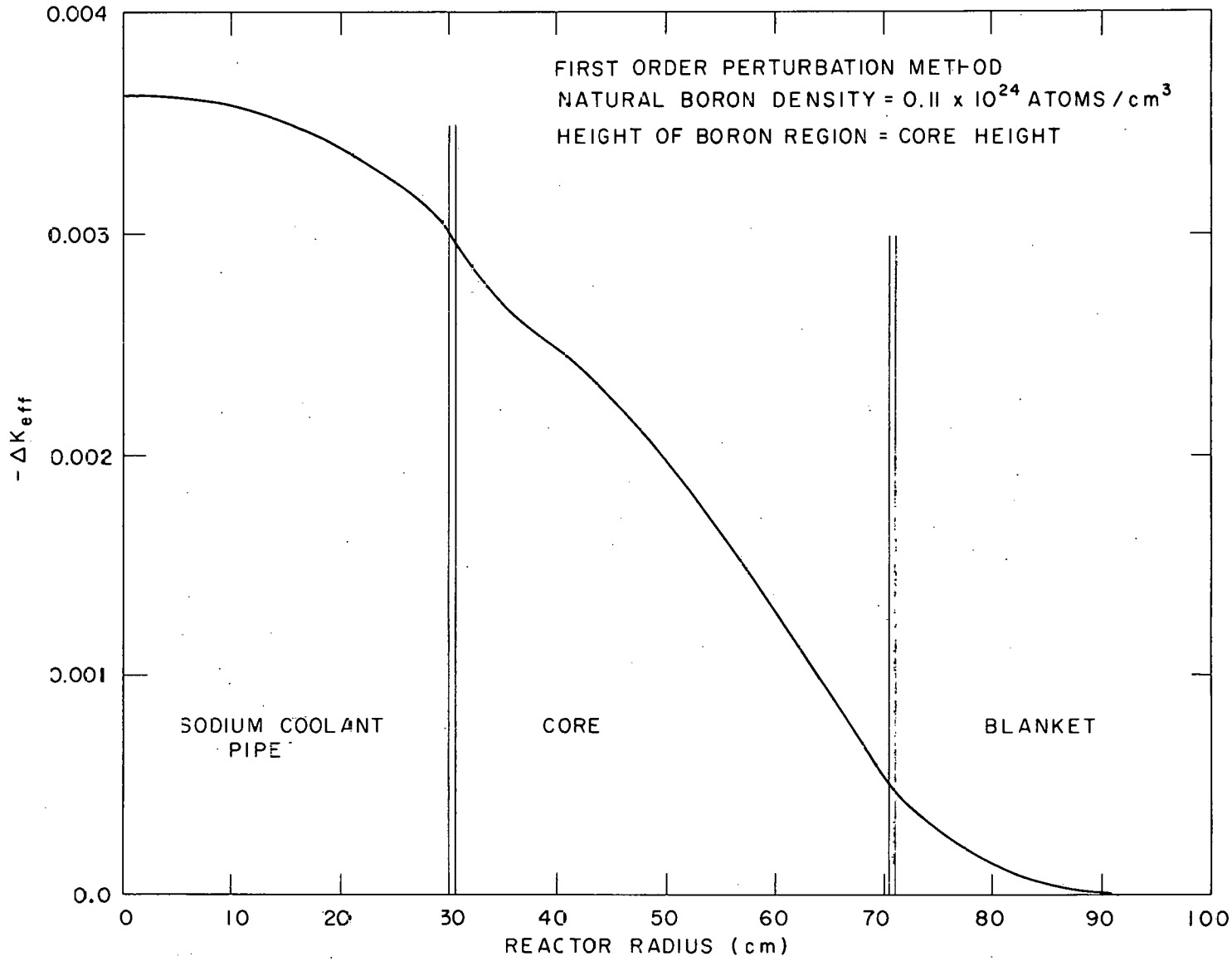

Figure 22. Reactivity worth of natural boron absorber per unit area as a function of position - radial flow oxide fuel.

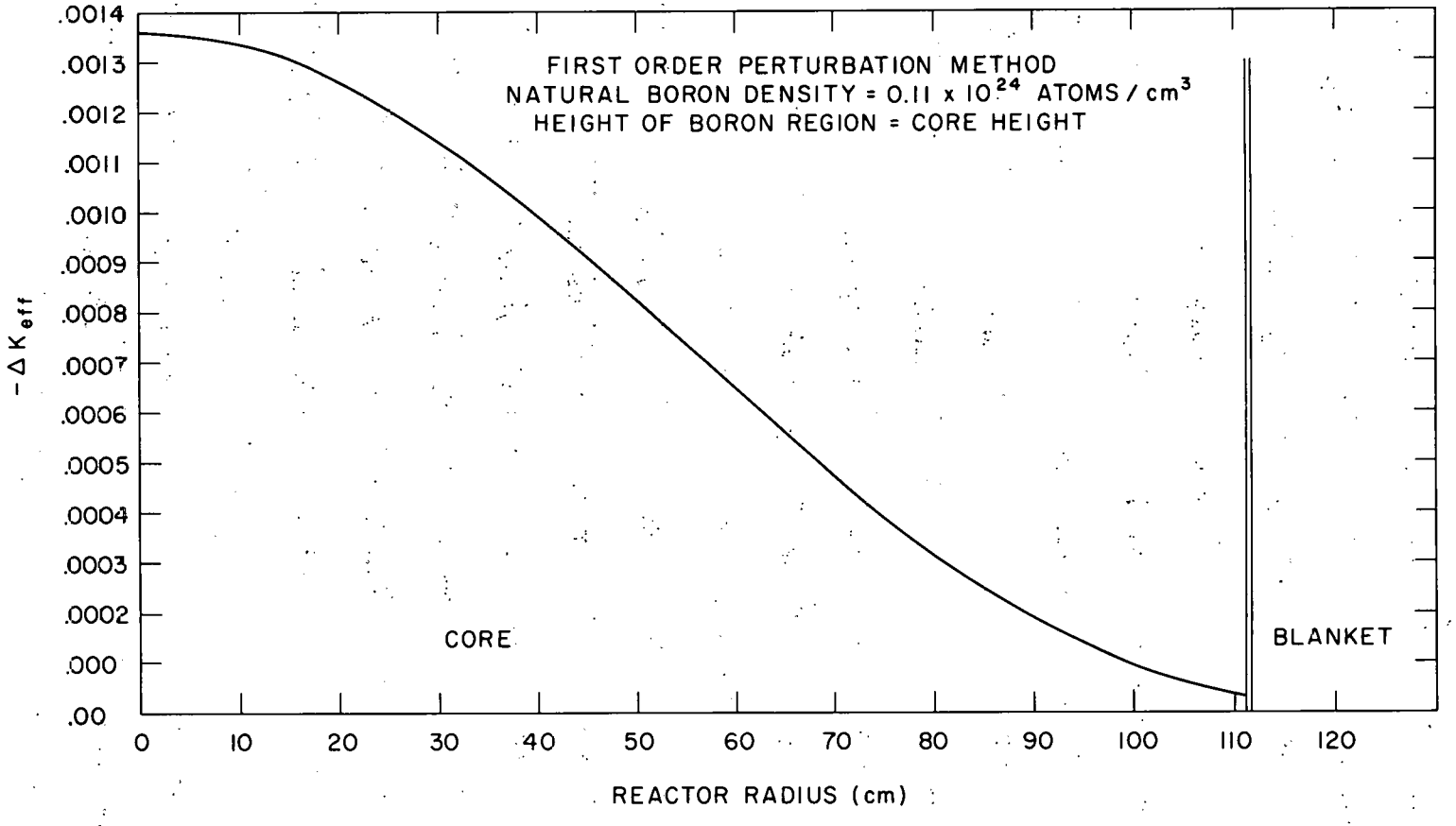

Figure 23. Reactivity worth of natural boron absorber per unit area as a function of position - axial flow carbide fuel.

designs. Yiftah and Okrent examined the sodium reactivity coefficient as a function of reactor size and composition[10]. Some general remarks will be made concerning this effect. The sodium reactivity coefficient may be resolved into three separate components due to changes in absorption, leakage and the neutron spectrum. The absorption component results simply in an increase in reactivity with decreasing sodium density due to the decrease in parasitic absorption in sodium. This component is usually much smaller in magnitude than either of the others and not significant. Reduction in sodium density results in a hardening of the spectrum because there is less of a material that is responsible for a considerable degradation of the neutron energy spectrum. The loss of sodium also causes an increase in leakage since the neutrons undergo fewer collisions in the reactor. The relative importance of these effects depends on a number of parameters including the size of the reactor. In a large reactor the leakage is generally small, and increased leakage due to decreased sodium density will not be important. Therefore, the hardening of the spectrum and the resultant increase in reactivity (due both to an increase in Y^{49} with energy and increased fast fission in U^{238}). will be the overriding component. In small reactors a decrease in sodium density will have its strongest effect in increasing leakage, and reactivity will decrease.

Results of calculations of k_{eff} vs sodium density for the

reactors in this study are presented in Figure 24. These calculations were done by reducing sodium density uniformly throughout the reactor (core, blanket and sodium coolant pipe). In Figure 24, ρ is the value of sodium density relative to the density at operating conditions ρ_o. Values of $k_{eff}(0)$ are those computed in cylindrical geometry with the fuel loading for a nominal k_{eff} of 1.01. From an examination of Figure 24 it is seen that for both the carbide fueled and oxide fueled radial flow reactors reactivity decreases as sodium density is reduced. No calculation was performed for the no sodium case because of the difficulty of taking into account the large void (empty coolant pipe) which exists at the center of the reactor under that condition. The decrease in reactivity with decreasing sodium density is to be expected since these are small reactors and in addition have an especially large amount of leakage due to the central coolant pipe. The carbide fueled radial flow reactor, being smaller than the oxide fueled, experiences a more rapid decrease in reactivity. The axial flow carbide reactor has a larger volume little leakage and experiences an increase in reactivity as sodium density decreases.

The sodium density coefficient as calculated here may be interpreted in various ways. It may represent a coefficient for loss of coolant in the case of a rupture of the coolant line. In this case the approximation must be made that the loss of coolant may be adequately represented by a uniform decrease in sodium den-

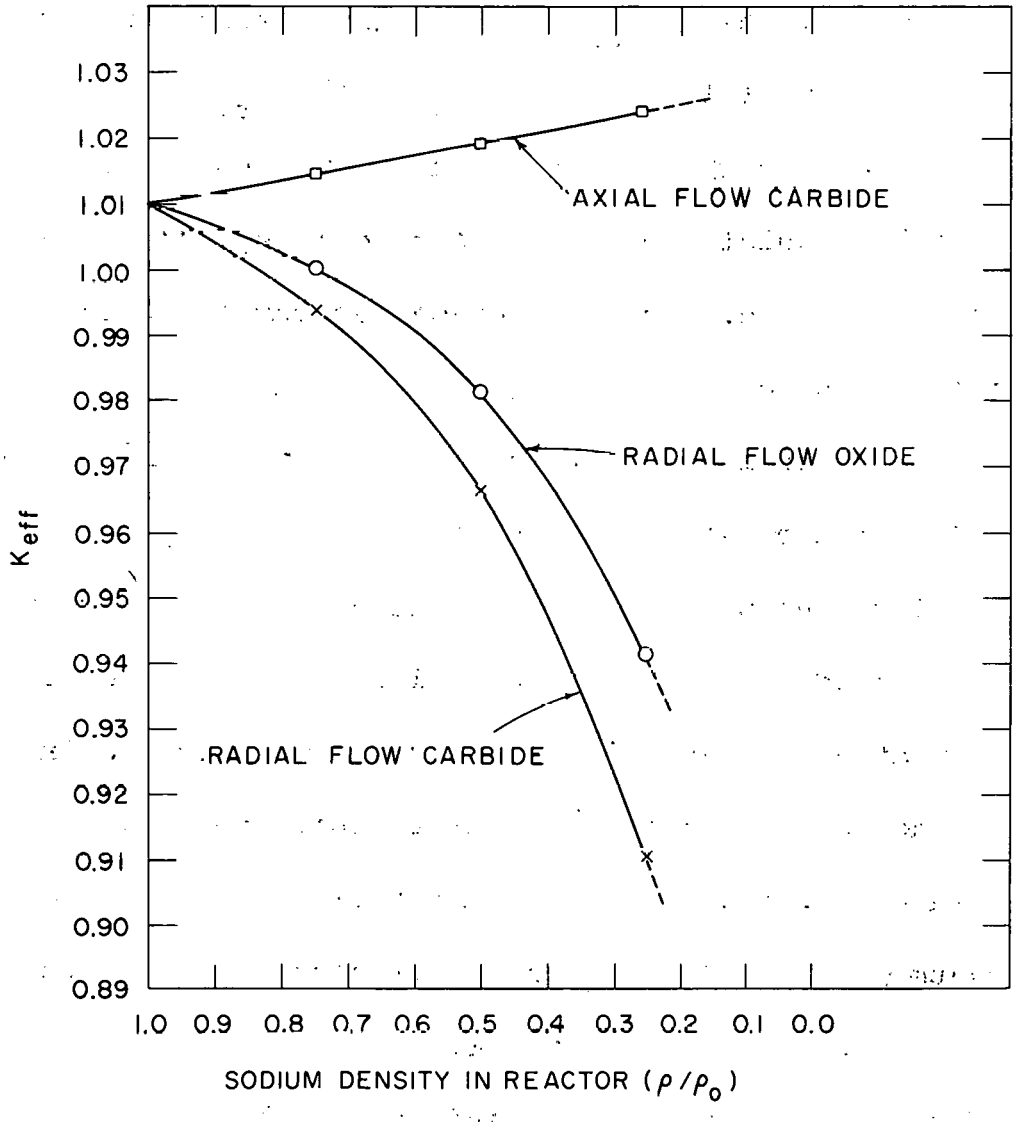

Figure 24. K_{eff} vs. density of sodium in reactor.

sity in the reactor when in fact the loss of coolant would most probably result in a lowering of the coolant level. The decrease in sodium density can represent voids in the coolant because of boiling caused by local hot spots or the presence of cover gas bubbles in the coolant. The sodium coefficient may also be considered as the sodium temperature coefficient of reactivity. In that case it is necessary to interpret the coefficient in terms of the change of sodium density with temperature. A decrease of 10% in sodium density corresponds to a rise in sodium temperature of $\sim$ 350°C or 630°F[14]. Since the effective delayed neutron fraction of the axial flow carbide fueled reactor is $\sim$ 0.004, a change in sodium temperature of $\sim$ 350°C would not cause this reactor to become prompt critical .

The sodium coefficients derived from Figure 24 were used to prepare Table 10 . The values presented there are given in terms of

$$- \frac{\Delta k_{eff}/k_{eff}(o)}{\Delta \rho / \rho_o} ,$$

that is the change in k_{eff} relative to the value with full density sodium divided by the change in sodium density relative to the full density. The sign convention that results from this definition of the coefficient for the reduction of sodium density is such that a minus sign for the coefficient indicates a decrease in reactivity with a decrease in sodium density. Since the curves in Figure 24

TABLE 10

SODIUM COEFFICIENTS FOR SETTLED BED FAST REACTORS

$$\left(- \frac{\Delta k_{eff}}{k_{eff}(o)} \Big/ \frac{\Delta \rho}{\rho_o} \right)$$

	Sodium Density Change		
Reactor	1.00 → 0.75	1.00 → 0.50	1.00 → 0.25
Radial Flow Carbide	-0.0644	-0.0872	-0.1318
Axial Flow Carbide	+0.0182	+0.0186	+0.0185
Radial Flow Oxide	-0.0394	-0.0564	-0.0916

are not linear, values of the coefficients are tabulated as averages over several intervals all starting with full density sodium. In order to interpret the coefficient for reduction of sodium density in terms of a sodium temperature coefficient, it is necessary to assign a negative sign to the coefficient in order to make it conform to common usage.

Partial coefficients for a 25% reduction of sodium density in each region separately are shown for each of the three reactor types in Table 11 . In the two radial flow designs most of the contribution to the change in reactivity comes from the coolant pipe, since most of the leakage is from this region. In the axial flow design the increased leakage caused by a sodium density decrease in the blanket is much smaller in magnitude than the contribution to reactivity from spectral hardening caused by a decrease in sodium density in the core. Although the decrease in reactivity with decrease in sodium density that occurs in the radial flow cores is a desirable feature under certain conditions (it tends to make the reactor stable at full power operation), it will also introduce additional reactivity under conditions where sodium density increases.

Since for the radial flow designs the greatest reactivity contribution is due to changes that take place in the coolant pipe, an effort was made to determine if this effect could be reduced by

TABLE 11

EFFECT OF 25% DECREASE IN SODIUM DENSITY

(k_{eff} = 1.01 with full density sodium)

Reactor	Δk_{eff} Pipe Only	Core Only	Blanket Only	Whole Reactor
Radial Flow Carbide	-0.0140	-0.0007	-0.0013	-0.0160
Radial Flow Oxide	-0.0091	+0.0003	-0.0010	-0.0098
Axial Flow Carbide	-	+0.0047	-0.0002	+0.0045

varying the diameter of the pipe. A series of calculations were performed on the radial flow carbide fueled core for coolant pipes of varying radius, maintaining constant core volumes and keeping the height of the core equal to its outer diameter. The results of these calculations are shown in Figure 25 . The magnitude of the sodium coefficient can be reduced by reducing the diameter of the coolant pipe. Since the axial flow design has a coefficient that is opposite in sign, and the magnitude will decrease with decreasing core size, it is to be expected that by properly adjusting the size and configuration of these reactors it would be possible to design a reactor that has as small a sodium coefficient as desired.

Previously reported studies of the sodium coefficient have been confined to reactors whose geometry could reasonalby be described by one space dimensional analyses. Results of experimental measurements of sodium reactivity measurements are becoming available, as for example the ZPR-III Assembly 35 mockup of the Fermi B reactor core[15, 16]. At the same time attention has been paid to improved methods of taking into account elastic scattering resonances in light elements and the resultant perturbation of the neutron flux spectrum in the vicinity of these resonances[11,12]. These techniques have been applied to the calculation of sodium coefficients[13]. Any further work on the reactor design in the present report must include investigating the use of refined cross

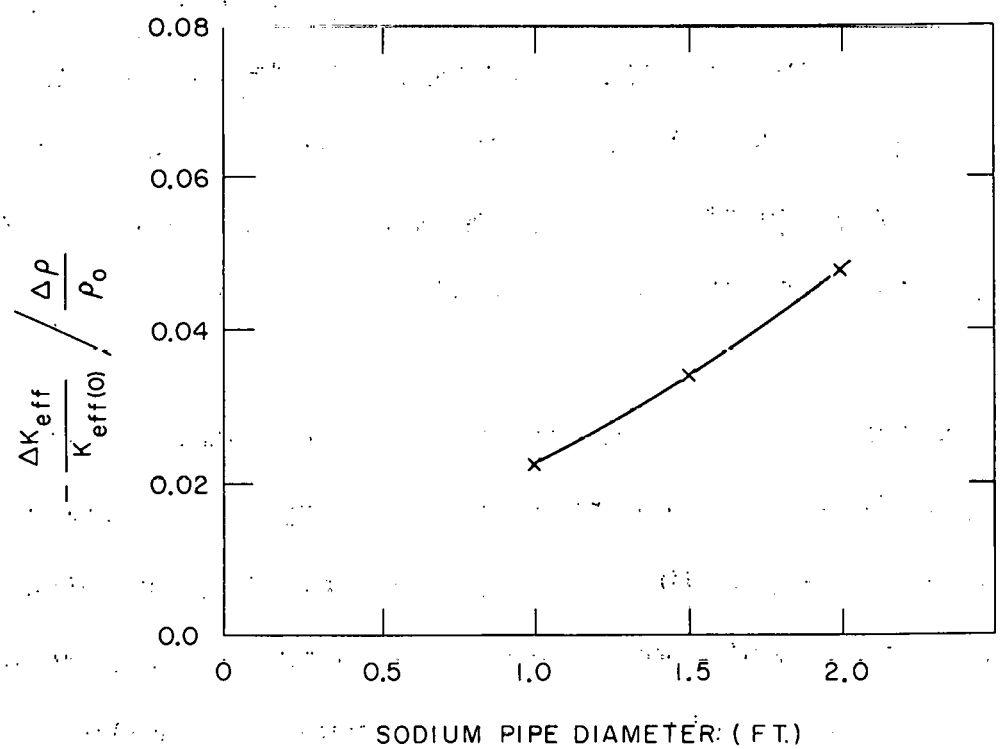

Figure 25. Sodium reactivity coefficient vs. sodium pipe diameter - radial flow carbide fuel.

section averaging methods for the sodium resonance scattering in predicting the measured reactivity changes in experimental assemblies, and if this method indicates an improved agreement with experimental results, it will be used in further calculations. Even more important that this, however, particularly for the radial flow designs, it is necessary to use a two dimensional analyses in order to adequately describe the system. The large leakage of neutrons down the coolant pipe is inadequately represented in one dimension, and the sodium reactivity coefficients obtained must be regarded as only preliminary.

One additional effect was investigated. This was the effect of sodium expulsion caused by settling of the bed. The case looked at, for all three reactor designs, was a change in the bed density from 60 volume precent of the core to 65 volume percent, and a consequent reduction in the sodium volume fraction from 40 volume percent to 35 volume percent. The settling included both the whole core, and the central ¼ of the core.

It was necessary to perform this calculation in slab geometry in order to get a reasonable model to represent the settling. In order to do this, the core in slab geometry was taken to have a radial leakage the same as that found in the cylindrical calculation. In order to obtain this with the best possible accuracy without a true two dimensional calculation, an iteration was performed on the leakages as described by the tranverse buckl-

ing in both the cylindrical and slab geometries. This was facilitated by the use of the Buckling Iteration Program[7,8] that was made available by Atomics International as an additional program with AIM-6. It was from this slab calculation that the ratio of maximum to average power generation rate in the axial direction was obtained.

Once the slab representative of the core in the axial direction was obtained, the height and composition of the various regions was adjusted to account for the settling. Sodium expelled from the core went into the pool above or below the core. The resulting reactivities were then calculated, and the results are shown in Table 12. It is seen that in all cases reactivity increases as a result of fuel compaction. Among the radial flow cases, the carbide fueled core, with its small volume is slightly more sensitive to fuel bed settling, while the axial flow reactor which is much larger than either of the radial flow designs experiences much less of an increase in reactivity for the same fractional bed settling. A local settling gives an effect proportional to the core affected and to the importance of the region affected. Thus a settling in the central ¼ of the core has an effect ½ as large as that for the whole core, and hence an importance per unit volume approximately twice the core averaged value. The results in Table 12 are given per percent volume change in sodium density, and are obtained by averaging over a -12.5% change

TABLE 12

EFFECT OF BED SETTLING FROM REFERENCE CONDITION

Reactor	$\frac{-\Delta k_{eff}/k_{eff}(o)}{\Delta V/Vo}$ for sodium volume fraction change of -12.5%	
	Change in whole core	Change in central ¼ of core
Radial Flow Carbide	+0.259	+0.124
Axial Flow Carbide	+0.0860	+0.0399
Radial Flow Oxide	+0.213	+0.104

in sodium volume fraction (40% to 35%). For any reactor, the reactivity change due to a given percentage change in sodium volume fraction is given by the tabulated result times the change in sodium volume fraction. Thus a change of sodium volume fraction in the whole core of the carbide fueled radial flow reactor from 0.400 to 0.396 would be a change of $0.01 = \delta V/V$ and the reactivity change would be $\delta k_{eff} = (+0.26)(0.01) = +0.0026$.

In these calculations of fuel particle settling, it was not possible to fully account for the important effect of radial leakage (particularly in the radial flow designs) by a one dimensional model. Therefore, the results presented must, like the calculations presented for the sodium coefficients in cylindrical geometry, be regarded as preliminary, to be refined by the use of two dimensional analysis.

ECONOMICS

Power Generation Costs

The power costs for the settled bed fast reactor presented in this section are still of a preliminary nature. Parametric type surveys of core physics, core fuel cycle and blanket reprocessing cycle must be performed before optimum costs can be obtained. The costs shown here are representative but should not be considered final. Overall cost trends for the two types (axial and radial) of fast reactors studied are best seen by referring to Figure 26 . This is a plot of fuel cycle and power generation costs versus core burnup. On the basis of burnup it is noted that the axial flow type core is lower in costs up to 73,000 MWD/MT burnup, but in excess of this burnup the radial flow oxide type is lower. The radial flow carbide core appears to have higher costs than the other cases for any equal burnup. There are a number of factors, namely breeding ratio, inventory, core size and the like which cause this, and since the differential is small it would be premature to select one type in favor of the other. Since fixed charges, operation and maintenance costs and nuclear insurance charges are all approximately equal for the cases considered, it is in fuel cycle costs that the differential appears. The axial core has an inventory of approximately two to three times the radial cores. One would thus expect the fabrication costs to be at least twice as much for the axial case. How-

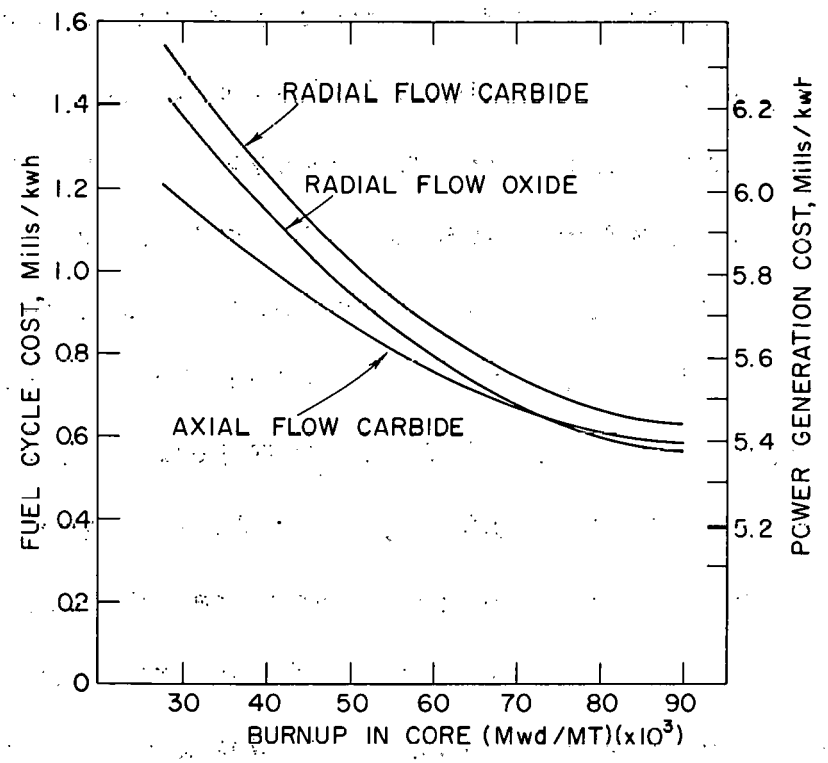

Figure 26. Fuel cycle and power costs vs. burnup.

ever, Figure 26 does not show the time it takes to reach a given burnup for each core type. The axial core has an initial breeding ratio of 1.39 versus 0.84 for the radial oxide and 0.76 for the radial carbide. This difference plus the large inventory yields a burnup of 30,000 MWD/MT in 45 months (operation) for the axial core as compared with 12 months for the radial oxide core and 8 months for the radial carbide core. The fabrication charges are thus written off over a much longer time period for the axial core, and are thus lowest for the axial case. At burnups over 60,000 MWD/MT fabrication and processing charges have become very small and fuel cycle costs are approaching the base use charges for each case.

Power generation costs in mills/kwh for the three cores studied are shown in Table 13. These costs are based on ~24 operating months core cycle time for the radial type and 45 months for the axial type which corresponds to burnups of 88,000 MWD/MT for the radial carbide core, 63,000 MWD/MT for the radial oxide core, and 30,000 MWD/MT for the axial core. The core cycle times were arbitrarily selected as representing reasonable times very early in the study though it now appears that the radial carbide case at 88,000 MWD/MT may be unrealistic. The burnup numbers given throughout this report are maximum values. However, in reactors of this type where fuel is well mixed during a core cycle maximum burnup

TABLE 13

POWER GENERATION COSTS

mills/kwhr

	24 mo. Cycle Radial Flow Carbide	24 mo. Cycle Radial Flow Oxide	45 mo. Cycle Axial Flow Carbide
Fixed Charges	3.66	3.66	3.68
Fuel Cycle	0.62	0.75	1.16
Operation & Maint.	0.95	0.95	0.95
Nuclear Insurance	0.20	0.20	0.20
TOTAL	5.43	5.56	5.99

and average burnups are not very different. The costs presented are in general below those given for the Advanced Plutonium Fueled Fast Breeder[1]. Capital costs are lower since the 1200°F sodium outlet temperature from the reactor permits the choice of a high efficiency turbine generator plant. The station efficiency is 42%. Fuel cycle costs are low due to high breeding ratio, high burnup and long fuel in-core residence times which reduce fabrication and chemical reprocessing charges. This applies to the blanket as well. The question of how to treat use charges in a breeder reactor is controversial but the effect of the use charge on total power cost is small (0.2-0.6 mills/kwh). Any change in the method of computing this charge would not greatly affect the final conclu-

sions of a preliminary estimate of this type.

Capital Costs

Since no detailed plant design has been made, it is neither feasible nor practical to carry out a detailed cost estimate. Hence for the turbine generator part of the plant a cost based on $70 per installed kilowatt was assumed. This cost is comparable with costs for an equivalent section of a high temperature, high pressure coal fired plant[2]. The reactor section of the plant was estimated at $35,000,000 using costs given for the Advanced Plutonium Fueled Fast Reactor[1]. Annual Fixed Charges are computed at the rate of 14.3% of all capital costs. A separate rate for nondepreciating capital costs such as land was not used since this refinement is beyond the accuracy of this cost estimate. Total plant cost is $64,000,000 which amounts to $178 per installed kilowatt.

Operation, Maintenance and Nuclear Insurance Costs

$2,400,000 per year or 0.95 mills/kwh has been allocated for operation and maintenance costs. The Cost Evaluation Handbook number for a 360 MWe plant which includes total labor, fringe benefits, maintenance materials and normal operating supplies as well as special operators for this type of plant amounts to $900,000 or 0.35 mills/kwh. An extra $1,500,000 or 0.6 mills/kwh has been added to account for the contamination of the primary loop and

fluid bed handling procedures for the fuel. The advanced plutonium fast breeder reactor at 300 MWe allocated $1,878,000 or 0.95 mills/kwh for operation and maintenance so that the use of 0.95 mills/kwh for the settled bed concepts which allows $522,000 more is not considered unreasonable.

Nuclear insurance costs consist of $60,000,000 liability coverage at an annual premium of $260,000, all risk property insurance at $220,000/yr and government indemnity at $26,000/yr. Total insurance is thus $506,000 per year or 0.2 mills/kwh.

Fuel Cycle Costs

Fuel cycle costs for three power reactor cases are presented. These are the radial flow carbide fueled core, the radial flow oxide fueled core and the axial flow carbide fueled core with height = 0.6 diameter. The costs have been calculated using the method outlined in the "Nuclear Power Plant Cost Evaluation Handbook", Volume 4. The design parameters used are those listed in the various tables of reactor characteristics. The operating and economic parameters which were used as the basis for the analyses are listed in Table 14 and Table 15.

The results of the calculation are given in Table 16 for 24 month operation of the radial cores and 45 months operation for the axial core. Again as in Table 13 on power generation costs these cases represent a wide difference in fuel burnup. Using

TABLE 14

OPERATING PARAMETERS

	Radial Flow Carbide	Radial Flow Oxide	Axial Flow Carbide
1. Plant Operating Factor, %	80	80	80
2. Shipping Time, AEC to Fabricator, days	20	20	20
3. Shipping Time, Fabricator to Reactor, days	20	20	20
4. Shipping Time, Recycle to AEC, days	20	20	20
5. Shipping Time, Reactor to Chem. Proc. Plant, days	20	20	20
6. Conversion and Fabrication Plant throughput rate MTU/month	4	4	4
7. Lead Time Before Charging Batch to Reactor, days	30	30	30
8. Spare Fuel, % of Core	4	4	4
9. Batch Size per Loading			
Core, MTU	5.96	8.4	35
Blanket, MTU	28.8	27.2	42.4
10. No. Batches per Chem. Processing Campaign	1	1	1
11. Losses During Fabrication, %	1.0	1.0	1.0
12. Losses, Conversion Pu, %	1.0	1.0	1.0
13. Losses, Chem. Separation Pu, %	1.0	1.0	1.0
14. Decay Cooling Period, days	120	120	120
15. Chem. Separation Plant Processing Rate, kg U	310	310	840
16. Residence Time in Reactor			
One Core Loading, calendar days	892	892	1650
One Blanket Loading, calend.days	1784	1784	3300

TABLE 15

ECONOMIC PARAMETERS

1.	Conversion and Fabrication Cost (Exclude shipping, use charges and losses) $/kg U	60
2.	Shipping Charge, AEC to Fabricator, $/kg U	1.50
3.	Shipping Charge, Fabricator to Reactor, $/kg U	1.50
4.	Shipping Charge, Reactor to Chem. Process, $/kg U	16
5.	Shipping Charge, Chem. Process to AEC, $/kg U	1
6.	Use Charge, %/yr	4.75
7.	Pu Price, $/g (metal)	9.50
8.	Conversion Charge, U Nitrate to UF_6, $/kg U	5.60
9.	Conversion Charge, Pu Nitrate to Pu Metal, $/g	1.50
10.	Separations Plant Daily Charge, $	17,000

TABLE 16

FUEL CYCLE COSTS
mills/kwhr

	24 month Radial Flow Carbide	24 month Radial Flow Oxide	45 month Axial Flow Carbide
Core			
1. Fabrication	0.06	0.08	0.18
2. Shipping	0.02	0.03	0.06
3. Chem. Processing	0.33	0.43	0.51
4. Pu Use Charge	0.20	0.24	0.62
5. Pu Consumption or Credit	0.34	0.28	-0.15
Subtotal	0.95	1.06	1.22
Blanket			
1. Fabrication	0.15	0.15	0.11
2. Shipping	0.05	0.05	0.04
3. Chem. Processing	0.12	0.12	0.07
4. Pu Use Charge	-	-	-
5. Pu Credit	-0.64	-0.63	-0.28
Subtotal	-0.32	-0.31	-0.06
Net Fuel Cucle Cost	0.63	0.75	1.16
Total Less Use Charge	(0.43)	(0.51)	(0.54)

table 16 in conjunction with Figure 26 permits one to see the effect of burnup on the fuel cycle cost.

The fabrication costs for both oxide and carbide fuel spheres are assumed to be $60/kg U. It is recognized that handling recycle plutonium will require remote fabrication techniques and that this is further complicated by "always safe" handling procedures necessitated by working with uranium "enriched" with ~10% plutonium and that all this will certainly increase the fabricating costs over an estimated $30/ kg U cost for producing low enriched uranium ceramic pellets. However, it is felt that it should be possible with metric ton requirements to develop methods for fabricating these simple ceramic shapes that will not be much higher in cost than the UO_2 pellets being manufactured at the present time. It is of interest to determine the effect of higher fabricating costs on the fuel cycle cost for a typical case. If we assume that the fabrication charge is a factor of 3 too low and is thus $180/kg U rather than $60/kg U then fabrication costs in mills/kwh at 63,000 MWD/MT burnup for the radial carbide, radial oxide and axial carbide cores increases by 0.16, 0.16, and 0.18 mills/kwh respectively. Fuel cycle costs thus increase from 0.82, 0.75, and 0.72 mill/kwh to 0.98, 0.91 and 0.90 mills/kwh respectively. Even at this level the fuel cycle costs are quite low.

The use charge was calculated on the basis that all

fresh fuel was leased from the AEC and all bred fuel removed from the reactor was sold to the AEC. Hence a use charge was applied to all fuel added to the reactor and no use charge was applied to material bred in the reactor. The reasoning used in not applying inventory charges on bred plutonium while it is in the reactor is analogous to an oil or coal mine operator who does not apply inventory charges to his oil or coal until it is taken from the ground and put into storage. Since the blanket has a large volume, attempts at short time interval removal of bred plutonium would result in exorbitant chemical processing costs. Monthly mixing of the blanket material maintains the blanket breeding ratio and distributes bred plutonium uniformly throughout the volume.

Interest on fabrication capital has been neglected since its effect on the fuel cycle cost is generally less than 0.05 mills/kwh. In calculating chemical processing costs it was assumed that fuel which is U-238 containing Pu-239 could be processed at the same throughput as a U-238 fuel enriched with an equivalent amount of U-235.

TABLE 6

TABLE OF REACTOR CHARACTERISTICS

A. Identification of Reactor

1.	Name of reactor	Directly Cooled Fast Reactor			
		Axial Flow (height=diam)	Axial Flow (height=0.6 diam)	Radial Flow (carbide)	Radial Flow (oxide)
2.	Thermal power (in core), Mw +	838	837	824	824
	Blanket (7% of core) Mw	59	59	57	57
3.	Net electrical power output, Mw	363	363	359	359
4.	Neutron spectrum	fast	fast	fast	fast
5.	Coolant material	sodium	sodium	sodium	sodium
6.	Fuel: Material	UC-PuC	UC-PuC	UC-PuC	UO_2-PuO_2
	Form	0.265-in. spheres	0.225-in. spheres	0.122-in. spheres	0.080-in. spheres
7.	Blanket: Material	UC	UC	UC	UO_2
	Form	0.250-in. spheres	0.250-in. spheres	0.125-in. spheres	0.150-in. spheres
8.	Distinguishing Features	Coolant is in intimate contact with the fuel in the core and blanket			
9.	Plant Type Being Described	Conceptual designs of full-scale plants for cost evaluation purposes			

TABLE 6 (continued)

	Axial Flow (height=diam)	Axial Flow (height=0.6 diam)	Radial Flow (carbide)	Radial Flow (oxide)
B. Engineering Data				
1. Reactor Vessel				
Design pressure, psi			200	
Design temperature, °F			1200	
Outside diameter, ft			6.93	
Over-all height, ft			13.75	
Wall thickness, in.			1.75	
Material			A.I.S.I. 316 SS	
2. Reactor Core Vessel				
Design pressure, psi			200	
Design temperature, °F			1200	
Inside diameter, ft			3.85	
Over-all height, ft			5.0	
Wall thickness, in.			0.5	
Material			A.I.S.I. 316 SS	

TABLE 6 (continued)

	Axial Flow (height=diam)	Axial Flow (height=0.6 diam)	Radial Flow (carbide)	Radial Flow (oxide)
B. Engineering Data (continued)				
3. Reactor Core				
Active diameter, ft	6.95	7.29	3.85*	4.63*
Active height, ft	6.95	4.37	3.85*	4.63*
Volume, ft^3	264	165	32.6	63.1
Composition				
UC-PuC (60%)	158.4	99	19.6	37.9**
Na (40%)	105.6	66	13.0	25.2
4. Reactor Blanket				
Radial thickness, ft	1.5	1.5	1.5	1.5

* Core contains 24 in. diam coolant pipe running along its axis.

** UO_2-PuO_2

TABLE 6 (continued)

	Axial Flow (height=diam)	Axial Flow (height=0.6 diam)	Radial Flow (carbide)	Radial Flow (oxide)
B. Engineering Data (continued)				
5. Primary Cooling System Core				
Number of flow loops	1	1	2	2
Flow per loop, gpm	34,500	34,500	17,000	17,000
Size of flow headers, in.	24	24	24	24
Material of construction	A.I.S.I. 316 SS	A.I.S.I. 316 SS	A.I.S.I. 316 SS	A.I.S.I. 316 SS
Total pressure drop, psi	182	114	70*	93*
Total pumping power (at 70% efficiency), hp	5,250	3,300	2,000*	2,640*

* The total pressure drop, pumping power, and flow velocity values are for the core only. The pressure drop and pumping power for both core and blanket are about 50% greater, and the average coolant velocity through both core and blanket is about 25% lower.

TABLE 6 (continued)

	Axial Flow (height=diam)	Axial Flow (height=0.6 diam)	Radial Flow (carbide)	Radial Flow (oxide)
B. Engineering Data (continued)				
6. Primary Cooling System, Blanket				
Estimated pressure drop, psi	-	5.44	45	-
Estimated head required to circulate Na through bed, ft	-	15.05	125	-
Estimated average flow velocity, ft/sec	-	0.27	2.09	-
C. Heat Transfer				
1. Coolant material	sodium	sodium	sodium	sodium
2. Inlet temperature, °F	550	550	550	550
3. Outlet temperature, °F	1200	1200	1200	1200
4. Coolant flow rate, lb/hr	1.44×10^7	1.44×10^7	1.42×10^7	1.42×10^7
5. Number of passes	1	1	1	1
6. Average flow velocity, ft/sec	2.25	2.02	1.84*	1.70*

* The total pressure drop, pumping power, and flow velocity values are for the core only. The pressure drop and pumping power for both core and blanket are about 50% greater, and the average coolant velocity through both core and blanket is about 25% lower.

TABLE 6 (continued)

	Axial Flow (height=diam)	Axial Flow (height=0,6 diam)	Radial Flow (carbide)	Radial Flow (oxide)
C. Heat Transfer (continued)				
7. Average volumetric heat generation rate in fuel bed, Mw/ft^3 bed (includ. voids)	3.17	5.07	25.3	13.05
8. Maximum volumetric heat generation rate in fuel bed, Mw/ft^3 bed (includ. voids)	10.95	16.55	52.8	28.1
9. Heat transfer surface, ft^2	43,000	31,700	11,550	34,000
10. Average heat flux, Btu/hr-ft^2	6.67×10^4	9.02×10^4	2.44×10^5	8.26×10^4
11. Maximum heat flux, Btu/hr-ft^2	2.29×10^5	2.94×10^5	5.08×10^5	1.78×10^5
12. Average fuel particle internal temperature difference, °F	24.9	28.9	42.2	68.7
13. Maximum temperature at center of fuel particle, °F	2018	2022	1689	1742
14. Maximum thermal stress on particles, psi	10,000	10,000	10,000	10,000

TABLE 6 (continued)

	Axial Flow (height=diam)	Axial Flow (height=0.6 diam)	Radial Flow (carbide)	Radial Flow (oxide)
C. Heat Transfer (continued)				
15. Maximum-to-average radial power power peaking factor	1.86	1.85	1.19	1.22
16. Maximum-to-average axial power peaking factor	1.48	1.41	1.40	1.41
17. Over-all power peaking factor	2.77	2.61	1.67	1.72
18. Hot channel factor	1.17	1.17	1.17	1.17
19. Factor to compensate for local variations in heat transfer coefficient over particle surface	1.25	1.25	1.25	1.25
20. Maximum sodium temperature, °F	1965	1960	1615	1622
21. Average core power density, kw/liter core (incl. void)	112	179	893	462
22. Average specific power in fuel, kw/kg Pu	-	300	1015	750

TABLE 6 (continued)

	Axial Flow (height=diam)	Axial Flow (height=0.6 diam)	Radial Flow (carbide)	Radial Flow (oxide)
D. Physics				
1. k_{eff}		1.01	1.01	1.01
2. U^{238}/Pu^{239} Ratio		12.57	7.34	7.67
3. Fuel Loading (kg Pu^{239})		2783	812	1096
4. Partial Breeding Ratio (core)		1.3742	0.7612	0.8458
5. Partial Breeding ratio (radial blanket)		0.1393	0.5387	0.4296
6. Partial Breeding Ratio (axial blanket)		0.1691	0.1912	0.1389
7. Total Breeding Ratio		1.6826	1.4911	1.4143
8. Median Fission Energy, kev		316	346	239
9. Average Capture to Fission ratio in Pu^{239}		0.2521	0.2309	0.2622
10. Radial Maximum to Average Power Generation Rate		1.91	1.19	1.25
11. Axial Maximum to Average Power Generation Rate		1.343	1.41	1.43
12. Average fast Flux in Core, neutrons/cm^2-sec		1.6×10^{15}	4.9×10^{15}	3.6×10^{15}

TABLE 6 (continued)

	Axial Flow (height=diam)	Axial Flow (height=0.6 diam)	Radial Flow (carbide)	Radial Flow (oxide)
D. Physics (continued)				
13. Core Breeding Ratio (average)		See Table 9	0.7098	0.796
14. Core Breeding Ratio (after 24 months)		" "	0.6639	0.748
15. Δk_{eff}/month (initial)		" "	-0.00458	-0.0027
16. Δk_{eff}/month (average)		" "	-0.00512	-0.0031
17. Δk_{eff}/month (after 24 months)		" "	-0.00566	-0.0035
18. Pu^{239} added/month (initial), kg		" "	7.85	6.4
19. Pu^{239} added/month (average), kg		" "	8.96	7.5
20. Pu^{239} added/month (after 24 months), kg		" "	10.14	8.5
21 Doubling Time (Pu^{239} only), years		15.6	5.8	9.2
22. Doubling Time (Pu, all isotopes), years		11.5	4.1	5.9
23. Effective Delayed Neutron Fraction		0.00399	0.00387	0.00379
24. Prompt Neutron Lifetime, sec		18.1×10^{-8}	22.4×10^{-8}	31.6×10^{-8}
25. Burnup - maximum at 24 months (45 months for axial)		30,000 MWD/MT	88,000 MWD/MT	63,000 MWD/MT

REFERENCES

Heat Transfer Section

1. BNL-5372 - Preliminary Report, internal distribution only

2. Leva, M., "Fluid Flow Through Packed and Fluidized Systems", Bulletin 504, U.S. Bureau of Mines, 1951

3. "Status Report for Sodium-Graphite Reactors", NAA-SR-Memo 4156, July 1959

4. "Preliminary Design of a 10-MW(t) Pebble Bed Reactor Experiment", ORNL-CF-60-10-63

Physics Section

1. H. P. Flatt and D. C. Baller, "AIM-6, A Multigroup Diffusion Equation Code", Computer Code Abstract No. 21, Nuc. Sci. and Eng., 11, No. 1, p. 102, Sept. 1961

2. P. Michael, BNL Internal Memorandum, April 1961

3. W. B. Loewenstein and D. Okrent, "The Physics of Fast Power Reactors", Proc. 2nd UN Intern. Conference on Peaceful Uses of Atomic Energy, Vol. 12, p. 16, Geneva 1958

4. P. Greebler, H. Hurwitz Jr., and M. L. Storm, "Statistical Evaluation of Fission Product Absorption Cross Sections of Intermediate and High Energies", Nuc. Sci. and Eng. 2, No. 3, p. 334, 1957

5. Reactor Physics Constants, ANL-5800, July 1958

6. S. Yiftah, D. Okrent, P. A. Moldarer, Fast Reactor Cross Sections, Pergamon Press, New York 1960

7. H. P. Flatt, "The Fog One-Dimensional Neutron Diffusion Equation Codes", NAA-SR-6104, August 15, 1961

8. A. Foderaro, "An Iteration Method for the Specification of Multigroup Buckling", Nuc. Sci. and Eng. 6, No. 6, p. 514 1959

Physics Section (continued)

9. J. B. Nims and P. F. Zweitel, "Sodium Temperature Coefficients in Fast Reactors", Trans. Am. Nuc. Soc., 2, No. 2, 1959 See also APDA-135

10. S. Yiftah and D. Okrent, "Some Physics Calculations on the Performance of Large Fast Breeder Power Reactors", ANL-6122, December 1960

11. H. H. Hummel and A. L. Rage, "Calculation of Effect of Elastic Scattering by Light Elements in Fast Reactors", Trans. Am. Nuc. Soc., 3, p. 273, 1960

12. H. H. Hummel and A. L. Rage, "An Accurate Treatment of Resonance Scattering in Light Elements in Fast Reactors", Proc. of the Seminar on the Physics of Fast and Intermediate Reactors, Vienna 1961

13. M. G. Bhide and H. H. Hummel, "Reactivity Coefficients of Sodium in Fast Assemblies", Proc. of the Seminar on the Physics of Fast and Intermediate Reactors, Vienna 1961.

14. Liquid Metals Handbook, Sodium (NaK) Supplement, TID-5277, July 1955

15. Argonne National Laboratory Reactor Development Program Progress Report, October 1961, ANL-6454

16. Argonne National Laboratory Reactor Development Program Progress Report, November 1961, ANL-6473

Economics Section

1. A. Amorosi and J. G. Yevick, "Data on Status of Fast Reactors", July 13, 1959

2. Federal Power Commission,"Steam Electric Plant Construction Costs", 12th Supplement F.P.C. S-143

ACKNOWLEDGMENTS

In addition to the authors, H. Susskind, Ira Thierer, J. Chernick, and T.V. Sheehan contributed to the effort. Richard Capello, Senior Designer, Burns and Roe, Inc., prepared the final drawings of the reactor.

We also wish to thank D. del Castillo for preparing the manuscript, and Robert Brown and George Cox for aid in reproducing this report.